MILLIMETER WAVE OPTICAL LINK/FREQUENCY CONVERTER SYSTEM

Tracor Aerospace Electronics Systems, Inc.

Ronald T. Logan, Jr. and R. Dale Bynum

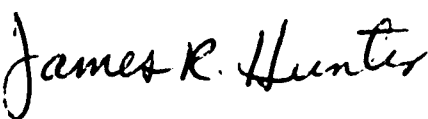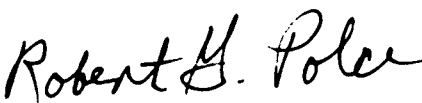**AIR FORCE RESEARCH LABORATORY
SENSORS DIRECTORATE
ROME RESEARCH SITE
ROME, NEW YORK**

This report has been reviewed by the Air Force Research Laboratory, Information Directorate, Public Affairs Office (IFOIPA) and is releasable to the National Technical Information Service (NTIS). At NTIS it will be releasable to the general public, including foreign nations.

AFRL-SN-RS-TR-1998-160 has been reviewed and is approved for publication.

APPROVED: *James R. Hunter*

JAMES R. HUNTER
Project Engineer

FOR THE DIRECTOR: *Robert G. Polce*

ROBERT G. POLCE, Acting Chief
Rome Operations Office
Sensors Directorate

If your address has changed or if you wish to be removed from the Air Force Research Laboratory Rome Research Site mailing list, or if the addressee is no longer employed by your organization, please notify AFRL/SNDR, 25 Electronic Pky, Rome, NY 13441-4515. This will assist us in maintaining a current mailing list.

Do not return copies of this report unless contractual obligations or notices on a specific document require that it be returned.

REPORT DOCUMENTATION PAGE

Public reporting burden for this collection of information is estimated to average 1 hour per response, including the time for reviewing instructions, searching existing data sources, gathering and maintaining the data needed, and completing and reviewing the collection of information. Send comments regarding this burden estimate or any other aspect of this collection of information, including suggestions for reducing this burden, to Washington Headquarters Services, Directorate for Information Operations and Reports, 1215 Jefferson Davis Highway, Suite 1204, Arlington, VA 22202-4302, and to the Office of Management and Budget, Paperwork Reduction Project (0704-0188), Washington, DC 20503.

1. AGENCY USE ONLY *(Leave blank)*	2. REPORT DATE	3. REPORT TYPE AND DATES COVERED
	Jul 98	Final Sep 95 - Sep 97

4. TITLE AND SUBTITLE
MILLIMETER WAVE OPTICAL LINK/FREQUENCY CONVERTER SYSTEM

6. AUTHOR(S)

Ronald T. Logan, Jr. and R. Dale Bynum

5. FUNDING NUMBERS

C   - F30602-95-C-0053
PE - 62702F
PR - 4600
TA - P5
WU - 01

7. PERFORMING ORGANIZATION NAME(S) AND ADDRESS(ES)

Tracor Aerospace Electronics Systems, Inc.
305 Richardson Rd.
Lansdale, PA 19446-1429

8. PERFORMING ORGANIZATION REPORT NUMBER

9. SPONSORING/MONITORING AGENCY NAME(S) AND ADDRESS(ES)

Air Force Research Laboratory/SNDR
25 Electronic Pky
Rome, NY 13441-4515

10. SPONSORING/MONITORING AGENCY REPORT NUMBER

AFRL-SN-RS-TR-1998-160

11. SUPPLEMENTARY NOTES

AFRL Project Engineer: James R. Hunter, SNDR, 315-330-7045

12a. DISTRIBUTION AVAILABILITY STATEMENT

Approved for public release; distribution unlimited.

12b. DISTRIBUTION CODE

13. ABSTRACT *(Maximum 200 words)*

Direct frequency conversion between mmW frequencies and baseband frequencies in the optical domain were validated. The technique utilized a dual wavelength phase locked laser system feeding an external Mach Zehnder modulator. The frequency difference between the two laser lines act as the local oscillator (LO) that up/down converts between baseband frequencies and millimeter wave frequencies. Additional work was performed to examine an alternate conversion technique that would eliminate the radio frequency and LO feed through on the output of the fiber optic link. In addition, the technique could increase the usable dynamic range by allowing more of the current saturating the photodetector to be from the signal and increasing the third order intercept point by 6 dB.

14. SUBJECT TERMS

Optical Frequency Converter, Optical RF Links, Optical Upconverter/Downconverter

15. NUMBER OF PAGES
56

16. PRICE CODE

17. SECURITY CLASSIFICATION OF REPORT	18. SECURITY CLASSIFICATION OF THIS PAGE	19. SECURITY CLASSIFICATION OF ABSTRACT	20. LIMITATION OF ABSTRACT
UNCLASSIFIED	UNCLASSIFIED	UNCLASSIFIED	UL

SUMMARY

The millimeter wave frequency converter subsystem (mmWFCS) contract was awarded to Tracor AES (formerly AEL) to validate direct frequency conversion between mmW frequencies and baseband frequencies in the optical domain. The technique utilized a dual wavelength phase locked laser system feeding an external Mach Zehnder modulator. The frequency difference between the two laser lines act as the local oscillator that up/down converters between baseband frequencies and millimeter wave frequencies.

Initial performance of the contracted work was performed at Tracor. Due to a turn over in personnel, a subcontract was issued to UTP in Lansdale to complete the validation of the mmWFCS concept.

The first section of the final report is a copy of the final report prepared by UTP under subcontract to Tracor (SFT57000G). The theory of operation, performance predictions, and summarized test results are included in their report.

Additional work was performed by Tracor to examine an alternate conversion technique that would eliminate the RF and LO feed through on the output of the fiber optic link. In addition, the technique could increase the usable dynamic range by allowing more of the current saturating the photodetector to be from the signal and increasing the 3rd order intercept point by 6 dB. Analysis and test data on this alternate technique is presented in Appendix A.

Each major section of the report; the UTP report and the appendix, contain a summary of the material contained in it.

TABLE OF CONTENTS

1. EXECUTIVE SUMMARY

This Final Report documents the theoretical and experimental results obtained by Uniphase Telecommunications Products (UTP) for a wideband photonic heterodyne frequency conversion system operating from 500 MHz to 40 GHz. The system studied consists of a low phase-noise optical heterodyne local oscillator (LO) generator derived from two phase-locked diode-pumped Nd:YAG lasers, a millimeter-wave lithium-niobate Mach-Zehnder modulator, and a high-speed photodiode. The sum and difference frequency products between the optical LO and the input RF signal to the Mach-Zehnder modulator are generated upon photodetection, yielding up-converted and down-converted products. An analysis of photonic heterodyne frequency conversion is presented, and experimental results are presented that are in good agreement with the theoretical prediction of 6 dB conversion loss.

This Report is structured as follows: First the motivation for and the background of photonic frequency conversion is discussed. Next, the heterodyne photonic frequency converting system is described. A review of the theory of photonic downconversion is presented from which the important RF parameters of interest to a system designer are computed, including conversion loss, noise figure, and dynamic range. Experimental frequency conversion results are presented and compared with the theory. Finally, a discussion of the experimental results and functional use and limitations of a photonic frequency converter are presented.

The emphasis of the theoretical and experimental characterization is on the performance of the heterodyne photonic frequency converter in terms of traditional RF performance parameters including gain, intercept points, noise figure, dynamic range, and phase noise. The experimental studies verify the theoretical model, therefore, the model developed here can be used to evaluate the heterodyne photonic mixing concept for system applications.

2. MOTIVATION AND BACKGROUND

Millimeter-wave (>30 GHz) systems with reduced front-end complexity, improved sensitivity, and greater dynamic range are desired for many communications, radar, and radio-science applications. To achieve the highest sensitivities, typical millimeter-wave systems incorporate local-oscillator (LO) generation and down-conversion in the front-end area. The bandwidth and dynamic range limitations of electronic mixers and amplifiers typically necessitate multiple stages of frequency conversion in sub-octave bands to achieve the required system performance, as shown in Figure 1. Problems associated with this architecture include: stable generation of multiple LO signals, re-radiation of LO power from the antenna due to poor RF-LO isolation of mixers, and reduced dynamic range due to cascading of multiple stages of downconversion.

The architectures of most RF, microwave, and millimeter-wave front end areas in existence today have a canonical block diagram, illustrated in Figure 1, that includes a low-noise amplifier and immediate down-conversion to a lower frequency IF for distribution to a remote processing area. The deficiencies of metallic cables and electronic mixers are the fundamental reason why this architecture has evolved to its present form. Down-conversion at the front-end area is necessary if maximum sensitivity is to be achieved, since coaxial cables or waveguide structures have increased skin effect losses with increasing frequency. This necessitates a complex front-end area requiring local oscillator distribution and possibly multiple stages of electronic down-conversion to shift the incoming millimeter-wave signal to a suitable IF band for processing by the receiver. This arrangement is incompatible with the size, power, and weight constraints of many systems, and is expensive to implement. Since the skin-effect losses of metallic cables are a fundamental physical limit, only the elimination of metallic cables can be expected to result in simplified front-end architectures for RF, microwave, and millimeter-wave systems. Also, diode mixers have limited operating bandwidths, due to the difficulty of impedance matching all three mixer ports over wide bandwidths to achieve acceptable VSWR and port-to-port isolation.

The advantages of the optical fiber transmission medium for microwave and millimeter-wave signal distribution are numerous. The CW laser source frequency is approximately 2×10^{14} Hz, so for a millimeter-wave modulation at a frequency of 100 GHz, the fractional bandwidth used in the transmission medium is only one part in 10^4. Because of this, the optical fiber medium has extremely wide inherent bandwidth by analog standards, with no measurable loss versus RF frequency slope, and low dispersion. Also, once the microwave signal is modulated onto an optical carrier, wide-bandwidth optical amplifiers can be used as gain stages, which have very flat gain versus frequency characteristics from RF through sub-millimeter-wave frequencies.

3. PHOTONIC FREQUENCY CONVERSION SYSTEM

In addition to signal transmission and amplification, optical waveguide devices may be used to perform RF frequency conversion [1,2,3]. An optical intensity modulator multiplies the input optical intensity with the input RF signal, to produce sum and difference frequencies upon photodetection. This type of system can simplify the front-end area of a mm-wave receiving system, as shown in Figure 2. In conventional (non-frequency converting) fiber optic links employing external modulation, the input signal is typically held constant, so the output intensity is just proportional to the voltage input to the modulator. However, if the input optical intensity is time-varying, the output intensity will be the multiplication of the input intensity envelope with the input RF voltage. If the input intensity envelope is a sinusoid, then the output intensity waveform contains sum and difference frequency products of the RF and LO waveforms. Photonic modulators used as mixers also offer greatly improved bandwidth and LO-RF isolation, chiefly due to the electrical decoupling of the mixer ports by the optical carrier which relaxes the impedance matching constraints typical of diode mixers.

Two optical modulators may be connected in series to obtain an optical frequency converting link [2]. However, the harmonic distortion and optical loss of the modulators limits the usefulness of this technique. In this Report, we investigate theoretically and experimentally the heterodyne photonic frequency converting fiber-optic link [1] in terms of RF system parameters. We calculate the RF to IF conversion loss, noise figure, and dynamic range of the photonic mixer, and present preliminary measurements at microwave and millimeter-wave frequencies.

The detailed block-diagram of the photonic downconvertor that was analyzed and tested is illustrated in Figure 3. The system consists of two diode-pumped Nd:YAG laser sources (Lightwave Electronics, Inc. Model 125) which are offset-locked in frequency to generate the optical heterodyne local oscillator signal, and a high-frequency electro-optic traveling-wave Mach-Zehnder modulator fabricated in $LiNbO_3$. A high-frequency photodiode is used to detect the optical output of the modulator. The photodiode linearly converts the time-varying optical intensity to electrical current. Modulation of the heterodyne optical LO source with the input RF signal in the Mach-Zehnder modulator produces sum and difference frequency products upon photodetection. The RF output power of these conversion products is then displayed on a spectrum analyzer.

3.1 Heterodyne phase-locked-loop operation

To maintain the laser offset frequency constant at 40 GHz, a millimeter-wave phase-locked-loop was constructed. The detailed construction of this loop is as indicated in Figure 3. The two laser outputs are combined in a 2x2 polarization-maintaining optical waveguide coupler with 50:50 coupling ratio. Each laser produces 23 dBm (200 mW) at 1319 nm. The output power from each port of the PM coupler is approximately 19 dBm for each frequency, for a total output power of 22 dBm.

One output of this coupler provides the input to the Mach-Zehnder modulator; the other output provides the heterodyne beat signal to the phase-locked-loop. The optical input to the phase-locked-loop is attenuated to 0 dBm and detected by a high-frequency HP 83440C photodiode. The output of the HP detector is not terminated internally, so a 3 dB pad is used at its output to provide matching to 50 ohms. The electrical heterodyne beat signal at the photodiode output is then amplified by a HP83051A 50 GHz amplifier, and 10 % of this signal is coupled out to monitor the offset frequency and measure phase noise. The 90 % output of the coupler is input to the RF input of the mixer. A 3 dB pad is used to improve the matching of the mixer input to 50 ohms.

The LO input of the mixer is driven by the HP83650B 50 GHz synthesizer, which provides the reference signal for the phase locked loop. This signal is offset in frequency by 400 MHz from the desired heterodyne beat signal, so that the IF output of the mixer is at 400 MHz. The IF output signal is adjusted in amplitude to be at -30 dBm at the input of the Lightwave Electronics Laser Offset Locking Accessory (LOLA) controller external signal input. The LOLA is operated in external mixer mode. It was found that if the input signal to the LOLA was too high, the amplifiers in the AGC circuit would overheat and cause the LOLA system to lose lock intermittently. If the input signal is kept to -30 dBm or less, this did not happen. For example, if the desired heterodyne beat frequency is 40.5 GHz, then the internal modes of the LOLA are setup as follows: external mixer: 40.5 GHz, external mixer IF: 400 MHz.

4. THEORY OF PHOTONIC HETERODYNE DOWNCONVERSION

In this section, we review the theory and derive expressions for photonic mixer conversion loss, noise figure, and dynamic range from the point of view of RF system design. In the frequency-converting fiber optic link considered here, the optical input to the Mach-Zehnder modulator is a dual-frequency laser, with frequency separation between the optical modes equal to the desired local oscillator (LO) frequency. The RF input signal modulates the intensity of this optical LO, producing sum and difference frequency products. The envelope of the optical LO intensity signal may be written

$$P_{LO}(t) = P_1 + P_2 + 2\sqrt{P_1 P_2}\, \cos(\omega_{LO}\, t + \phi_{12}(t))$$

where P_1 and P_2 are the output powers of the two laser modes with frequency difference ω_{LO} and relative phase fluctuation $\phi_{12}(t)$. Inserting this into the equation for the Mach-Zehnder modulator voltage-to-intensity transfer function obtains the modulator output at quadrature bias:

$$P_{out}(t) = \frac{P_{LO}(t)\alpha}{2}\left[1 - \sin\left(\frac{\pi\, V(t)}{V_\pi}\right)\right],$$

where α is the optical loss between the heterodyne optical output and the photodiode. We assume a sinusoidal RF input signal of the form $V(t) = V_o \sin(\omega_{RF}\, t)$ and we make the substitution $m = \dfrac{\pi\, V_o}{V_\pi}$, where V_π is the half-wave voltage of the modulator at the RF input frequency. Then, for $m < 0.1$, (i.e., linear approximation) the expression for the output time-varying optical power at the photodiode may be simplified to

$$P_{out}(t) = \frac{\alpha\, P_o}{2} + \frac{P_o\, m\alpha}{2}\sin(\omega_{RF}\, t) + \alpha\sqrt{P_1 P_2}\, \cos(\omega_{LO}\, t + \phi_{12}(t))$$
$$+ \frac{m\alpha\sqrt{P_1 P_2}}{2}\sin\left[(\omega_{LO} \pm \omega_{RF})t + \phi_{12}(t)\right]$$

where we have set the total DC optical power $P_o = P_1 + P_2$. The photodiode converts this signal linearly to current. The first term represents the DC photocurrent, the second term is at the RF signal frequency, the third is at the optical LO frequency, and the fourth are the upconverted and downconverted products. The phase noise of the optical LO and upconverted and downconverted signals given by $\phi_{12}(t)$ depends on the relative stability of the laser modes, to be discussed later.

4.1 Conversion Loss

We define the "conversion loss" for the photonic mixing process to be the ratio of the mixing term to the RF fundamental signal term. If the intensities of the two laser modes are equal, then $P_o = P_1 + P_2 = 2P$, and the conversion loss is calculated to be

$$C = \frac{\dfrac{m\alpha\sqrt{P_1 P_2}}{2}}{\dfrac{P_o\, m\alpha}{2}} = \frac{\sqrt{P^2}}{2P} = \frac{1}{2}.$$

Since the RF power is proportional to the square of the optical power, the conversion loss due to the optical mixing process is $20 \log(1/2) = 6$ dB. This additional conversion loss results in a 6 dB increase in link loss compared to a non-converting link. This theoretical conversion loss was verified in laboratory experiments at frequencies from baseband up to 40 GHz, to be discussed below.

The RF insertion loss for the downconverting link is defined as the ratio of the RF input power into the optical modulator to the RF output power delivered to the load. This is just the loss of a non-converting fiber optic link [4] plus the extra 6 dB loss due to downconversion just derived. The total loss of the converting link G_{conv} from RF input to IF output may be written

$$G_{conv} = \frac{\pi^2}{4} \frac{I_L^2 R_L R_m}{V_\pi^2}$$

where I_L is the portion of the photocurrent flowing in the load resistance R_L connected to the photodiode receiver, and the input impedance of the Mach-Zehnder modulator is R_m.

The half-wave voltage V_π is defined as the voltage at the RF input frequency w_{RF} required to produce an optical phase shift of π radians between the two arms of the Mach-Zehnder interferometer that comprises the intensity modulator. The calculated RF-IF gain for the converting link is plotted versus photocurrent in Figure 4 for modulator V_π of 1V and 10V, and load impedance R_L of 50 ohms and 1000 ohms. We note that the highest photocurrent of 10 amps shown in the plot is well beyond the limit of presently available microwave photodiodes. However, much larger photocurrents can be generated at baseband frequencies by using large-area photodiodes, and by combining their electrical outputs. For broadband microwave frequency photoreceivers, R_L is typically 50 ohms, and I_L is not necessarily equal to the dc average photocurrent flowing in the photodiode, but is typically one-half of the dc photocurrent due to the current divider between the internal matching resistance of the photodiode receiver and the load resistance of the following stage. However, at baseband, or in a narrow frequency range, it is possible to increase the load impedance to be greater than 50 ohms, resulting in improved link gain. Therefore, for high-frequency downconversion systems, the absolute

loss from RF input to IF output can be minimized by using a low-frequency large-area photodiode at the highest photocurrent possible, and matching the photodiode into the highest possible load impedance.

4.2 Linearity

The figure of merit for mixer linearity is the third-order intercept, which is defined as the point at which the power of the third-order intermodulation products generated in a two-tone intermodulation test would become equal to the fundamental output power. The linearity of the photonic downconverter is limited by the Mach-Zehnder modulator, so the distortion analysis is similar to the case of a non-converting link. The input third-order intercept point for a Mach-Zehnder modulator can be expressed as

$$IIP3_{mz} = \frac{4}{\pi^2} \frac{V_\pi^2}{R_m} \quad [\text{W}].$$

The input 1 dB compression point is 10 dB less than the input third order intercept point [4]. The output third-order intercept point of the downconverting link is the product of the RF link gain with the modulator input intercept point. In this case, the downconversion gain G_{conv} calculated above is used, yielding:

$$OIP3_{conv} = IIP3_{mz} G_{conv} = I_L^2 R_L \quad [\text{W}].$$

So the output third-order intercept point of the link depends only on the photocurrent and the load impedance. The dynamic range is therefore limited by the maximum photocurrent that the photodiode can handle. This is another motivation for using photonic downconversion instead of a non-converting fiber-optic link, since low-frequency photodiodes can have larger junction areas and therefore sustain larger photocurrents. This is plotted versus photocurrent for load impedance R_L of 50 ohms and 1000 ohms in Figure 5.

4.3 Noise

In a short link with low losses employing a shot-noise limited laser, such as the diode-pumped Nd:YAG lasers used in this study, the dominant output noise sources at microwave frequencies will be the shot noise generated in the photodetection process, and thermal noise generated in the resistor connected to the photodiode. The shot noise power density varies linearly with the detected photocurrent as

$$N_{total} = N_{shot} + N_{thermal} = 2eI_L R_L + kT \quad [\text{W/Hz}]$$

where e is the electron charge in coulombs. For photocurrents of more than 1 mA, the shot noise will typically exceed the thermal noise level generated in the output resistance

9

R_L. Of course, if other intensity noise exceeds the shot noise level, as is typically the case with relative intensity noise (RIN) in semiconductor lasers, then this must be taken into account.

For a frequency-converting link that uses lasers with negligible RIN noise, the equivalent input noise (EIN) of the converting link is equal to the input thermal noise at the modulator, plus the total output noise level divided by the RF-to-IF link loss:

$$EIN_{conv} = kT + \frac{N_{total}}{G_{conv}} = kT + \frac{8eV_\pi^2}{\pi^2 I_L R_m} + \frac{4kTV_\pi^2}{\pi^2 I_L^2 R_L R_m} \quad [\text{W/Hz}]$$

The EIN determines the minimum detectable signal level at the input to the Mach-Zehnder modulator. The noise figure of the photonic downconvertor is the difference in dB between the EIN and the thermal noise level at the input, which is assumed to be Johnson noise equal to kT. The noise figure of the photonic downconvertor is therefore given by:

$$NF_{conv} = 10\log\left(\frac{EIN_{conv}}{kT}\right) = 10\log\left(1 + \frac{8eV_\pi^2}{\pi^2 I_L R_m \, kT} + \frac{4V_\pi^2}{\pi^2 I_L^2 R_L R_m}\right) \quad [\text{dB}]$$

At high photocurrents when shot noise is dominant, the last term due to thermal noise is negligible, so the noise figure may be approximated as

$$NF_{conv} \cong 10\log\left(1 + \frac{8eV_\pi^2}{\pi^2 I_L R_m \, kT}\right) \quad [\text{dB}]$$

It is obvious from this expression that the noise figure for the converting link may be optimized by maximizing the photocurrent and modulator input impedance, and minimizing V_π of the modulator. The noise figure of the converting link is plotted in Figure 6 versus photocurrent for modulator V_π of 1V and 10V, and load impedance R_L of 50 ohms and 1000 ohms. It is noted that the input noise temperature of the photonic downconverting link becomes equal to the modulator temperature at high photocurrents.

4.4 Dynamic Range

The spurious-free dynamic range of the downconverting link is defined as the ratio of the output signal level to the output noise density when the third-order intermodulation products are equal to the noise level in a given bandwidth. This may be written as:

$$SFDR = \frac{20}{3}\log\left(\frac{OIP3_{conv}}{N_{total}}\right) = \frac{20}{3}\log\left(\frac{I_L^2 R_L}{2eI_L R_L + kT}\right) \quad [\text{dB-Hz}^{2/3}]$$

10

The spurious-free dynamic range of the photonic downconverting link versus photocurrent is shown in Figure 7. From this figure, it may be seen that the converting link SFDR depends only on the photocurrent in the shot-noise limited regime above approximately 1 mA. It is emphasized that this is the dynamic range of the entire downconversion chain from the input at microwave or millimeter-wave frequencies to the output at baseband. This should be compared to the dynamic range of an electronic downconverter chain that may require multiple mixing and amplification stages to convert a millimeter-wave input signal to a baseband IF signal, as in Figure 1. The spurious-free dynamic range in units of [dB Hz$^{2/3}$] can be converted to an SFDR in a given bandwidth B in units of [Hz] by the relation:

$$SFDR(B) = SFDR - \frac{20}{3}\log(B) \quad [dB].$$

For example, the SFDR of the photonic down-converting link is computed to be 110 [dB Hz$^{2/3}$] at a photocurrent of 10 mA. This corresponds to a SFDR in a 1 GHz bandwidth of

$$SFDR(1 \ GHz) = 110 - \frac{20}{3}\log(10^9) = 110 - 60 = 50 \quad [dB].$$

5. EXPERIMENTAL DOWNCONVERSION RESULTS

5.1 RF Link Loss

Experiments were carried out on the photonic downconverting system shown in Figure 3. The performance of the link, from the RF input to the RF output, was characterized extensively. The first parameter that was measured was the RF link gain from the RF input to the RF output. The setup used in the measurement is shown in Figure 8 and the results are shown in Figure 9. Also shown in Figure 9 is the response of the link with the frequency variations of the photodiode calibrated out. (This is equivalent to the response of the NRL Mach-Zehnder modulator versus frequency.)

Calibration of the photodiode is necessary because the theory presented in section 4 assumes that the responsivity of the photodiode is constant versus frequency. The two-laser optical LO source is used to measure the response of the photodiode. In a two laser system where the optical power of the lasers are equal, the theoretical signal level of the detected LO tone is given by

$$P_{rf} = 10\log\left(\frac{Z_L \times I_o^2}{2}\right) + 30 \quad \text{[dBm]}$$

where I_o is the current that flows in the load impedance Z_L. This level is independent of frequency, so by sweeping the frequency of the LO tone, it is possible to measure the actual frequency response of the photodiode. This measured response is then used to correct for the frequency response of the photodiode. The frequency response of the New Focus photodiode, measured using the LOLA system, is shown in Figure 10.

5.2 Conversion Gain

The ability of the link to upconvert or downconvert an input signal was measured. For the conversion gain measurement, an LO frequency of 40.5 GHz was used. The LOLA phase lock loop (PLL) system was used to phase lock the 40.5 GHz optically generated LO to an HP83650B signal generator at 40.1 GHz. (The IF frequency of the LOLA PLL was set to 400 MHz.) The measurement setup shown in Figure 8 was used to measure both the through response of the link (measurement frequency equals input frequency) and the converted response (measurement frequency equals the LO frequency minus the input frequency.) This measurement was performed for input RF signals from 0.5 GHz to 39.5 GHz at 0.5 GHz intervals. Figures 11a and 11b show the measured data after calibrating for the frequency response of the photodiode and the input cable. Figure 11a shows the block-upconversion of signals in the band RF = 0.5 GHz to 20 GHz to a frequency range of IF = 20.5 GHz to 40 GHz. Similarly, Figure 11b shows block down-conversion of signals in the band RF = 20.5 GHz to 40 GHz to a frequency range of IF = 0.5 GHz to 40 GHz. The "IF" frequency is the converted frequency, so that IF=LO-RF. Therefore, there is a spectral inversion of the signal block.

The amplitude difference between the measured RF and IF signal levels is equal to the

conversion gain of the link, as defined in Section 4. Figure 12 shows the measured conversion gain vers·is frequency. As predicted by theory of Section 4, the average of the conversion gain is 6 dB. The data has a standard deviation of 0.8 dB, which is within the published +/- 1.5 dB measurement accuracy of the spectrum analyzer.

5.3 Noise Figure

The dominant broadband source of noise in the two-laser photonic converting system was shot noise. It is this source of noise which sets the noise figure of the overall photonic converting system. The experimental setup shown in Figure 13 was used to measure the noise floor at the output of the photodiode. Figure 14 shows the measured noise floor data for the two-laser photonic converting system (LO frequency equals 45 GHz) with 3 mA photocurrent on a 1K ohm photodiode. This data is equal, within measurement accuracies, to the theoretical shot noise level for a 1 K ohm photodiode with 3 mA of photocurrent. If one of the Nd:YAG lasers is turned off, and the optical power on the photodiode adjusted to give 3 mA of photocurrent, the same shot noise level is measured. This is significant because it demonstrates that there is no serious degradation in the system noise floor due to the shot noise of the two lasers adding in phase, even when frequency-locked. If the laser's shot noise added in phase, there would be a 3 to 6 dB degradation in the measured noise floor. Since this effect is not observed, the assumption that the two laser sources produce uncorrelated shot noise is justified.

The measured output noise floor is used to compute the equivalent input noise figure. This was done by referring the measured output noise level back to the modulator input by subtracting the gain of the frequency-converting link, thus obtaining the equivalent input noise (EIN) of the link. The difference in dB between the EIN and thermal noise is the noise figure. Figure 15 shows the noise figure of both the non-converting and the converting link. This computation of noise figure is valid for frequencies in excess of 1 MHz from the IF frequency, and does not take close-to-carrier noise sources into account. Close-to-carrier noise will be discussed in detail later in the section on phase noise.

5.4 One dB Compression Point

The measurement setup shown in Figure 8 was used to measure the 1 dB compression point of the heterodyne photonic frequency-converting link. The frequency of the input RF signal generator was 4 GHz and the optical LO was set to 11 GHz. From a point where the link was not compressing (0 dBm RF input power), a reference measurement of the converting link gain was recorded at the RF input frequency and at both IF output frequencies of 7 GHz and 15 GHz. The RF input power to the modulator was then increased until the gain was reduced by 1 dB. Once this occurred, the RF input power level was then measured on the spectrum analyzer and recorded as the input 1 dB compression point. For the system shown in Figure 3, the measured 1 dB compression point was +15.85 dBm at the RF input frequency of 4 GHz. This value is the same for the non-coverting link as well as the converting link, since the compression point depends

13

only on the modulator. The 1 dB compression point versus frequency has the same relative frequency response as the link gain.

5.5 Output Third Order Intercept Point (OIP3)

A two-tone intermodulation distortion measurement was performed to quantify the third order intercept point, as shown in Figure 16. The photocurrent in the New Focus photodiode is 0.56 mA at 0 dBm incident optical power. Figure 17a shows the measured OIP3 for the lower side band of the upconverted signal as a function of optical LO frequency. The ripple in this response is due to the response of the photodiode verses frequency. As predicted by theory, the OIP3 of the converted link is 6 dB lower than the non-converted link.

The OIP3 was also measured for the downconversion case. For two input frequencies of 17.4 GHz and 17.6 GHz and an LO frequency of 16 GHz, the measured OIP3 for the non-converting link was measured to be -19.57 dBm and the converting link was measured to be -25.82 dBm. The difference between these measurements is 6.25 dB which is within measurement accuracies of the theoretical 6 dB value.

Taking the measured OIP3 at the photodiode and the link gain, the input IP3 was computed, see Figure 17b. In this figure it can be seen that the input IP3 increases with frequency. This effect is due to the modulator V_π increasing with frequency. The increase in V_π is seen both as an increase in link loss versus frequency and an increase in the input IP3.

The input 1 dB compression point of the system can be theoretically predicted from the IIP3 of the system. From Figure 12b, the IIP3 at 3 GHz is +25.6 dBm. From theory, the 1 dB compression point of a Mach-Zehnder interferometric modulator is 9.8 dB lower than the input IP3, or +15.8 dBm. A 1 dB compression point of +15.86 dBm was measured for the system, see Section 5.4, which is in excellent agreement with the measured input IP3 data.

5.6 VSWR

For the two-laser photonic conversion system shown in Figure 3, the input VSWR and output VSWR of the system is determined by the VSWR of the NRL Mach-Zehnder modulator and the New Focus photodiode, respectively. Figures 18 and 19 show the return loss of the NRL Mach-Zehnder and the New Focus photodiode, respectively. No special efforts were taken to optimize the VSWR of the modulator or photodiode. It is obvious that there is considerable room for improved impedance-matching of both devices. It is interesting to note that since the RF and IF ports are electrically isolated, they may be independently optimized over their respective operating frequency ranges. Therefore, no double- or triple-balancing, as is typically required in electronic mixers, is required to get good VSWR and isolation between ports of the photonic "mixer."

14

5.7 Relative Mixing Spur Level

One figure of merit of the performance of a frequency converting system is the level of the higher order harmonics produced by the frequency conversion components. In the system shown in Figure 3, the higher order harmonics were measured using the setup shown in Figure 8. For this test, an input frequency of 4 GHz at +6.82 dBm and an LO frequency of 11 GHz was used. Table 5.1 shows the frequency of the nth harmonic of the LO and the mth harmonic of the IF for the frequencies mentioned above. Table 5.2 shows the measured harmonic spurs levels after calibrating out the photodiode response versus frequency. Table 5.3 shows the relative levels of the spurs with respect to the response at 4 GHz. Notice that as theory predicts, there is a -6 dB conversion gain and that the dBc value between the 1st, 2nd, and 3rd harmonic is consistent.

RF\LO	0	1	2	3
-3	-	1	10	21
-2	-	3	14	25
-1	-	7	18	29
0	-	11	22	33
1	4	15	26	37
2	8	19	30	41
3	12	23	34	45

Table 5.1 Frequency of Harmonics

RF\LO	0	1	2	3
-3	-	-76.22	*(shaded)*	*(shaded)*
-2	-	-88.87	-103.23	*(shaded)*
-1	-	-41.51	-82.22	-101.3
0	-	-29.51	-73.63	-94.94
1	-35.21	-40.60	-81.25	-101.74
2	-83.33	-87.99	-99.73	*(shaded)*
3	-71.80	-76.35	*(shaded)*	*(shaded)*

Table 5.2 Measured Harmonic levels*
(Photodiode response calibrated out.)

RF\LO	0	1	2	3
-3	-	-41.02	*(shaded)*	*(shaded)*
-2	-	-53.67	-68.03	*(shaded)*
-1	-	-6.30	-47.01	-65.82
0	-	5.69	-38.43	-59.73
1	0.00	-5.40	-46.05	-66.53
2	-48.13	-52.78	-64.52	*(shaded)*
3	-36.60	-41.15	*(shaded)*	*(shaded)*

Table 4.7.3 Relative harmonic levels with respect to through response*.

* Shaded cells indicate measurement was limited by system noise floor.

5.8 Phase Noise

The setup shown in Figure 8 was also used to measure the RF phase noise of the heterodyne photonic frequency converting system at an LO frequency of 37 GHz. First, the RF phase noise of the phase-locked-loop reference signal generator at 37 GHz was measured using the phase noise utility software on the HP 8565E spectrum analyzer. Next, the photonic converting system was connected to the spectrum analyzer and the phase noise of the photodetected heterodyne LO signal was measured. Figure 20 shows the phase noise of the PLL reference signal generator, and the photodetected optical heterodyne LO signal.

The optical heterodyne LO signal has spurs at approximately 250 kHz and 500 kHz offset from the carrier. These spurs are most likely caused by the switching power supplies used in the LOLA PLL controller. (This conclusion was shared by the design engineer of the LOLA system.) The heterodyne LO signal phase noise is degraded from that of the reference signal generator at frequencies less than 10 kHz. This degradation is probably either due to noise in the PLL circuitry in the LOLA controller unit, or insufficient loop gain to bring the lasers into complete phase coherence with the reference generator at these frequencies.

A surprising result is that the phase noise of the heterodyne LO signal is lower than that of the reference signal generator for offset frequencies between approximately 20 kHz and 120 kHz. This is probably because the bandwidth of the PLL is approximately 10 kHz, and the phase noise of the lasers is simply lower than that of the reference generator at these offset frequencies. Theoretically, if the PLL has sufficient loop gain and adds no noise, the phase noise of the optical heterodyne signal should follow the phase noise of the reference generator for offset frequencies within the PLL bandwidth. From these results, it appears that there is room for improvement in the design of the PLL. However, redesigning the PLL was beyond the scope of this research effort.

Figure 21 shows the measured phase noise of the 1 GHz RF input signal generator, the detected optical LO signal at 37 GHz, and the upconverted signal at 38 GHz. As expected, the upconverted signal has the same phase noise as the optical LO signal. The higher phase noise at offset frequencies above 100 kHz is due to the limited signal-to-noise ratio of the detection circuitry at 38 GHz.

The phase noise of the converted signal is limited by the shot noise floor of the system. For offset frequencies greater than 100 kHz, the measured single side band phase noise has a floor of -100 dBc/Hz. For the input RF power level used in this experiment, the output signal level to noise ratio is 100 dB-Hz, which limits the measured phase noise to -100 dBc/Hz. Increasing the signal input level would increase the signal to noise ratio at the output, and increase the sensitivity of the measurement. From these results it can be seen that there is no serious degradation in the phase noise of the frequency-converted signal above the phase noise of the heterodyne optical LO signal at millimeter-wave

17

frequencies.   Therefore, as expected from the theory, it appears that the photonic frequency-conversion process adds no additional phase noise beyond that of the heterodyne LO.

6. DISCUSSION

From the calculations and measurements presented above, the photonic downconverting link has measured performance very close to the predictions of the theory derived here. Although the system measured in this research program has relatively high noise figure and link loss, the point of this research program was to develop a theoretical model of the photonic frequency-converting link, and verify the model with experiments. From the figures presented in the theory section, it can be seen that a noise figure of 10 dB and link loss of less than 5 dB can be achieved at a photocurrent of 70 mA into a 50 ohm load, with a modulator V_π of 1 V. This is beyond the current state of the art, but points to the need for further developments in modulator technology, as well as high-power photodiodes.

The full advantage of photonic downconversion can be appreciated only when the architecture of the entire downlink from millimeter-wave input to baseband output is considered carefully. Typical microwave receiver systems with input frequencies up to 20 GHz use two-stage downconvertors employing up to 20 separate components including mixers, amplifiers, filters, power dividers, limiters, etc. Millimeter-wave downconvertors may use three stages of mixing in a superheterodyne receiver system. Also, the first downconversion stage is usually located as close as possible to the antenna, so the first LO must be generated at this location. This is typically done by frequency multiplication of a lower-frequency reference signal in the front end area. In surveillance systems, radiation of the LO signal from the antenna must be minimized, but diode mixers typically have only 20 to 30 dB LO-RF isolation. Isolation of the front end amplifier and antenna from the LO signal requires additional components that deteriorate dynamic range and add complexity to the front-end area.

With the photonic downconverter approach, many of these problems are eliminated, since the optical LO generation can be performed near the IF processing equipment, and simply delivered to the modulator via an optical fiber. Then, only the antenna, an amplifier, preselecting filter and the modulator need to be located in the front-end area. Also, since the LO signal is optical, there is infinite LO-RF isolation, and no possibility of LO leakage from the antenna. At the present state of the art of optical modulators and photodiodes, significant front-end amplification, on the order of 40 dB or more, is necessary to offset the losses and noise figure of the photonic frequency converting system to achieve reasonable (< 20 dB) noise figures for a millimeter-wave downconversion system. However, the overall system simplification attainable by using the photonic downconversion approach may outweigh this disadvantage. With fewer components located in the harsh environment that many antennas must endure, overall system reliability is enhanced. Also, since the photonic mixer can convert millimeter-wave signals directly to baseband, there are fewer components in the entire downconversion chain that could possibly limit the dynamic range and reliability.

Besides the high loss, another disadvantage of the photonic downconverter approach is that there is theoretically no RF-to-IF or LO-to-IF isolation. In fact, the non-converted RF frequency is theoretically 6 dB higher than the converted IF signal. This means that both the input signal and the converted signal will appear at the photodiode (provided the frequency response of the photodiode is sufficient). For mixing applications that deal with LO, RF, and IF bandwidths that overlap, there is no isolation provided by the photonic mixing system, so other components would be necessary to achieve RF-to-IF or LO-to-IF isolation. For applications where the RF frequency band is significantly higher than the IF frequency band, a proper selection of the cutoff frequency of the photodiode would provide a level of RF-to-IF isolation. Also, the Mach-Zehnder modulator is not a single-sideband mixer, so a preselecting filter is required at the front-end to reject images.

In spite of these limitations, a Mach-Zehnder modulator coupled with an optical heterodyne LO generator as a photonic frequency-converting fiber optic link does offer interesting new architectural possibilities to the RF system designer. One of the most significant possibilities is the reduction of equipment in the front-end areas of receiving systems, which could reduce the components located in harsh environments, and eliminate the need for high-frequency photodiodes.

7. CONCLUSION

Theoretical and experimental results for a heterodyne photonic frequency-conversion system were presented. A theoretical model of the photonic downconversion system was developed from which pertinent RF parameters were calculated. Good agreement between the theoretical calculations and the experimental data was demonstrated. It was demonstrated that two commercially-available Nd:YAG ring lasers, operated in a PLL circuit, can achieve reasonable phase noise performance as an optical heterodyne LO source at millimeter-wave frequencies. However, much work needs to be done to realize a widely tunable optical heterodyne LO source with low phase noise, as well as optical modulators with higher sensitivity, and photodiodes capable of handling high optical power.

8. ACKNOWLEDGMENT

9. REFERENCES

1. R. T. Logan Jr., X. S. Yao, G. F. Lutes, "Photonic Signal Processing and Transmission," NASA/Jet Propulsion Laboratory New Technology Report, NPO 19437, 11 April 1994.

2. G.K. Gopalakrishnsn, W.K. Burns, C.H. Bulmer, "Microwave-optical mixing in LiNbO$_3$ modulators," IEEE Transactions on Microwave Theory and Techniques, Vol. 41, No. 12, December 1993.

3. M.J. Wale and M.G. Holliday, 21st European Microwave Conference Workshop, pp. 78-82, 1991.

4. X. S. Yao, G. F. Lutes, R. T. Logan Jr., L. Maleki, "Field Demonstration of X-Band Photonic Antenna Remoting in the Deep Space Network," JPL/NASA Telecommunications and Data Acquisition Progress Report, 42-117, January-March 1994, p. 29.
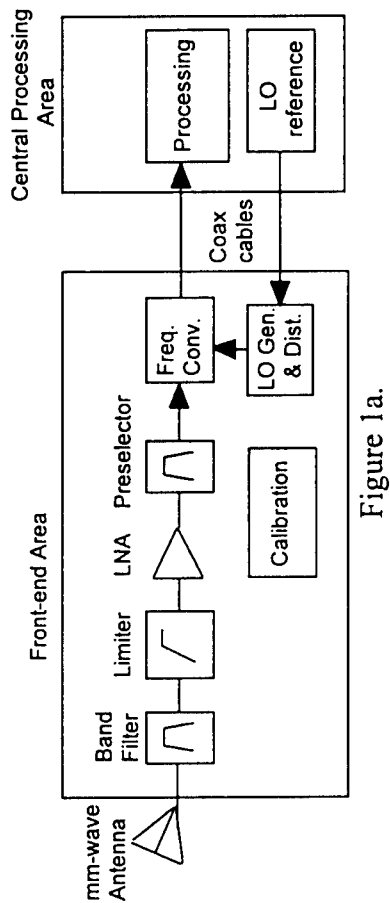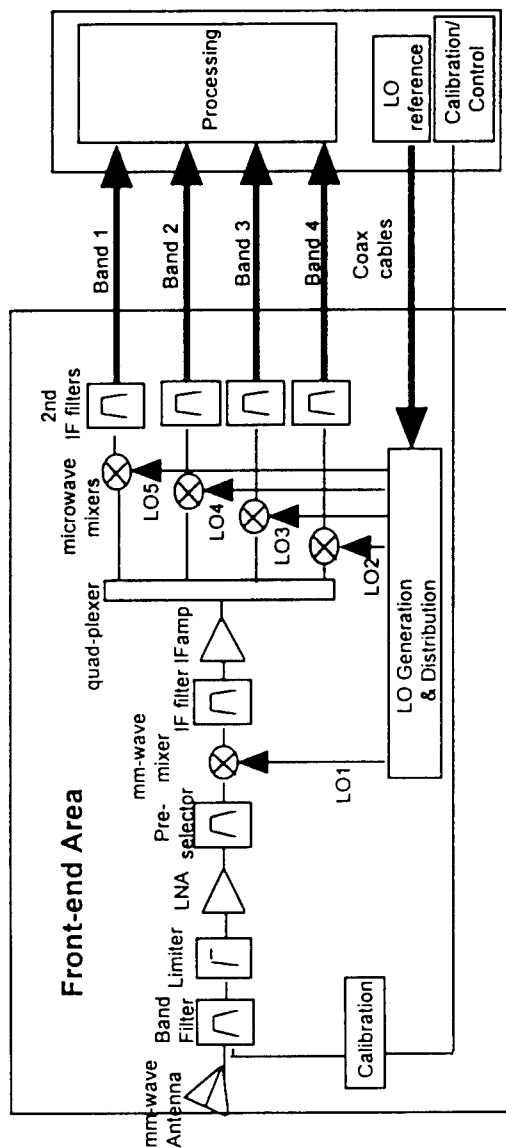
Figure 1a.

Fig. 1b.

Figure 1. Conventional microwave front-end architectures employing electronic downconversion:

a). simplified block diagram,

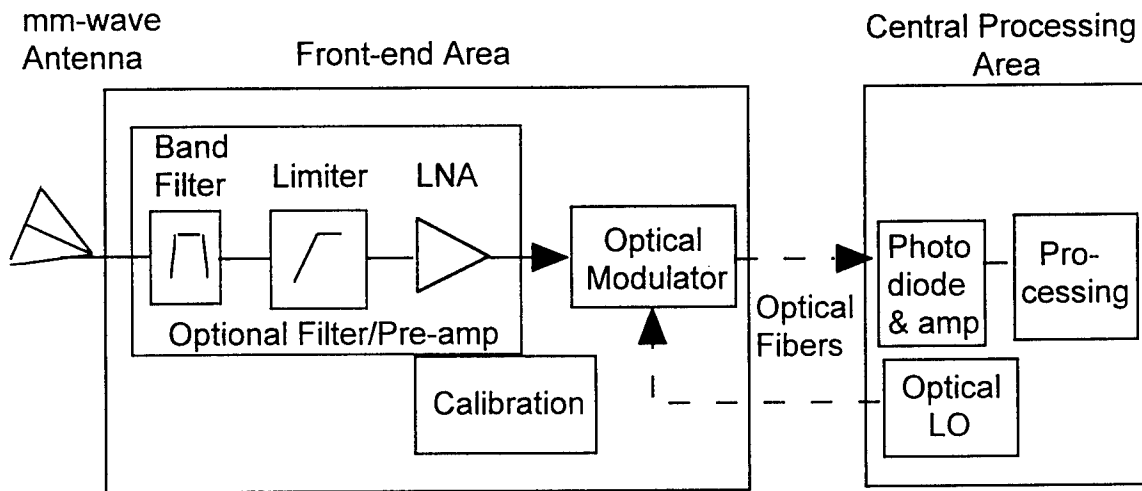b). expanded block diagram of mm-wave EW receiver front-end concept.

Figure 2. Simplified microwave front-end concept employing photonic downconversion.
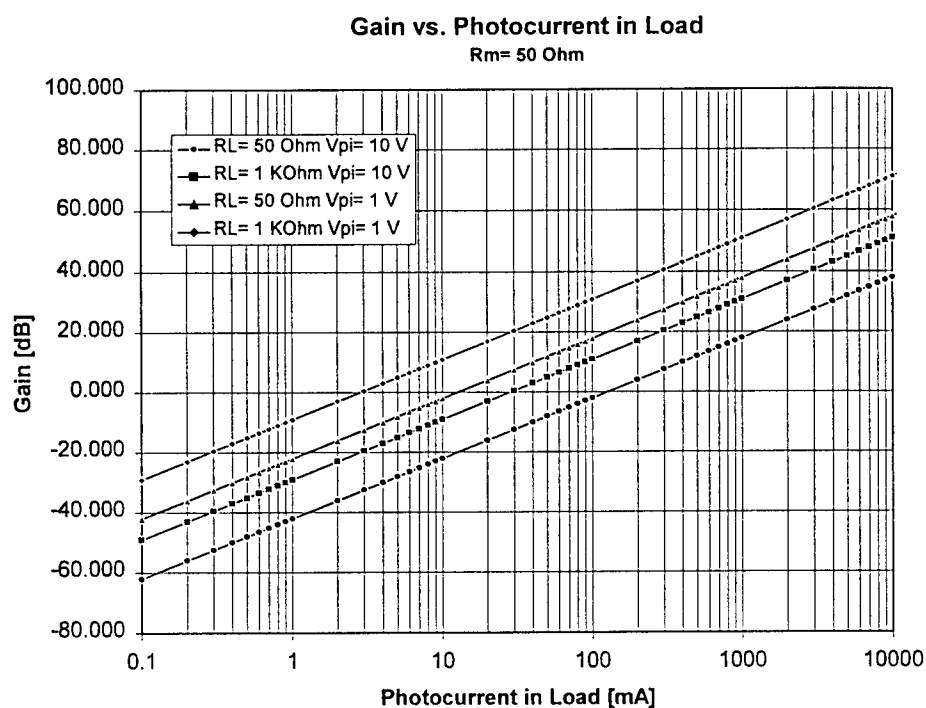
Figure 3. Two laser photonic converting system block diagram.

Gain vs. Photocurrent in Load
Rm= 50 Ohm

Figure 4   Theoretical Link Gain verses photocurrent in load for different V_π and load impedance values.

Output IP3 vs. Photocurrent in Load
Vpi=10 [V], Rm= 50 [Ohms]
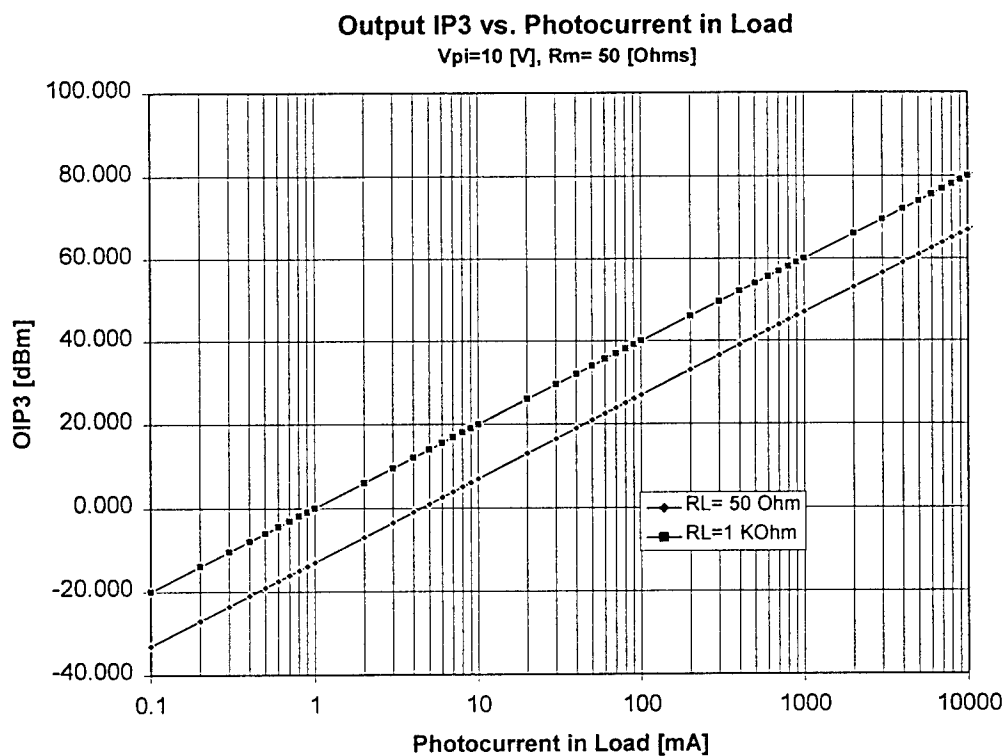
Figure 5   Theoretical Output IP3 verses photocurrent in load for different load impedance values.

Noise Figure vs. Photocurrent
Rm=50 Ohms

Legend:
- RL= 50 Ohm Vpi= 10 V
- RL= 1 KOhm Vpi= 10 V
- RL= 50 Ohm Vpi= 1 V
- RL= 1 KOhm Vpi= 1 V

Y-axis: Noise Figure [dB]
X-axis: Photocurrent in Load [mA]
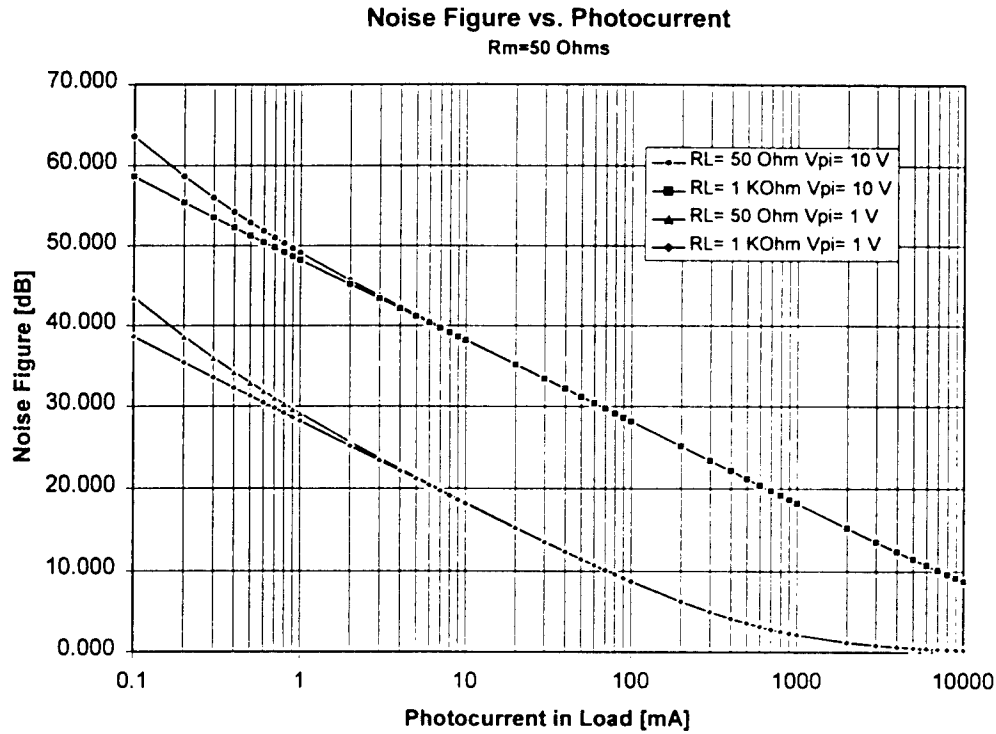
Figure 6   Theoretical Noise Figure verses photocurrent in load for different load impedances and V_π.

SFDR vs. Photocurrent

Legend:
- RL= 50 Ohms
- RL= 1KOhms

Y-axis: SFDR [dB Hz^2/3]
X-axis: Photocurrent in Load [mA]
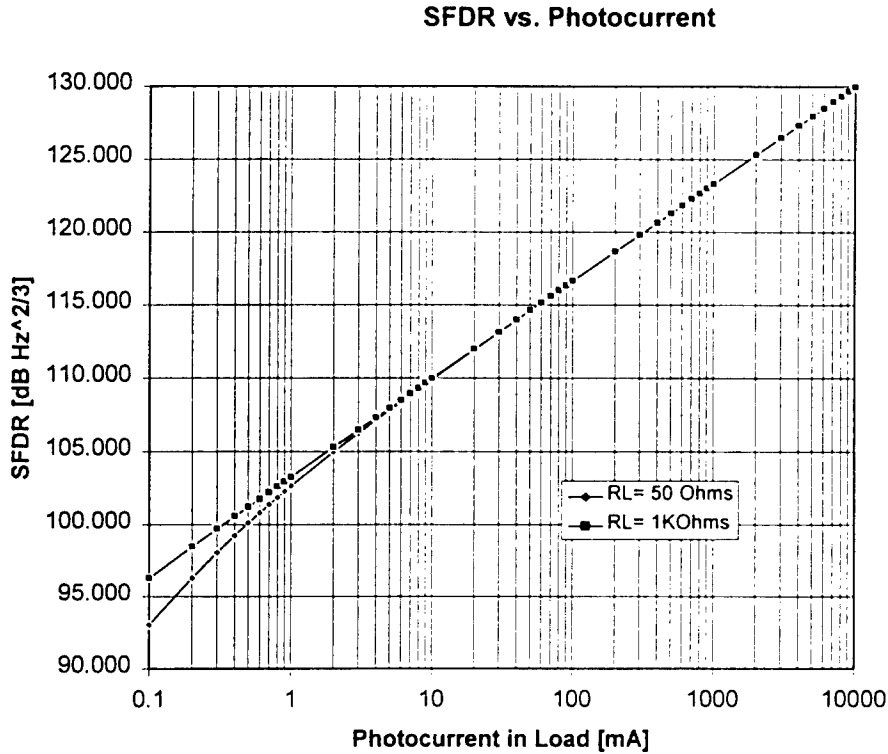
Figure 7   Theoretical Spur-Free-Dynamic Range verses photocurrent in load for different load impedances.
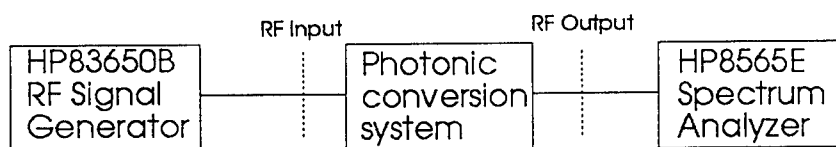
Figure 8. Measurement Setup for Conversion Gain.
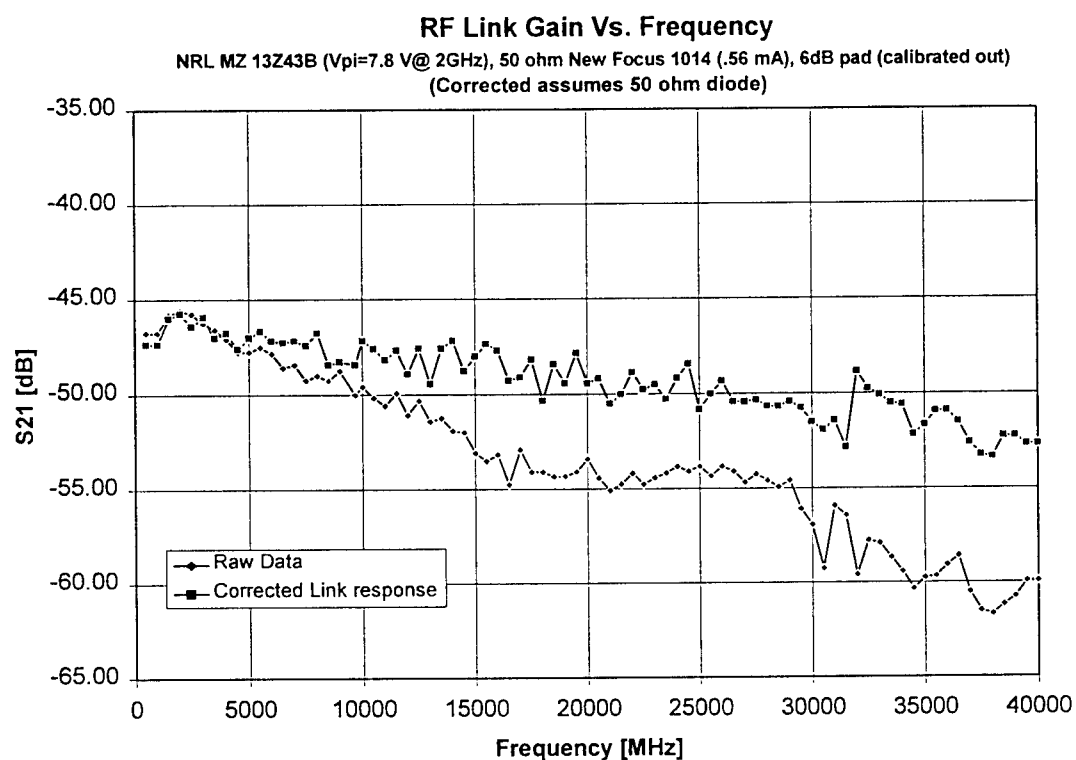
Figure 9. Non-Converting link gain with and without calibrating photodiode. Upper trace represents the actual frequency response of the NRL Mach-Zehnder modulator. The lower trace is raw data that represents the product of the modulator and photodiode frequency responses.
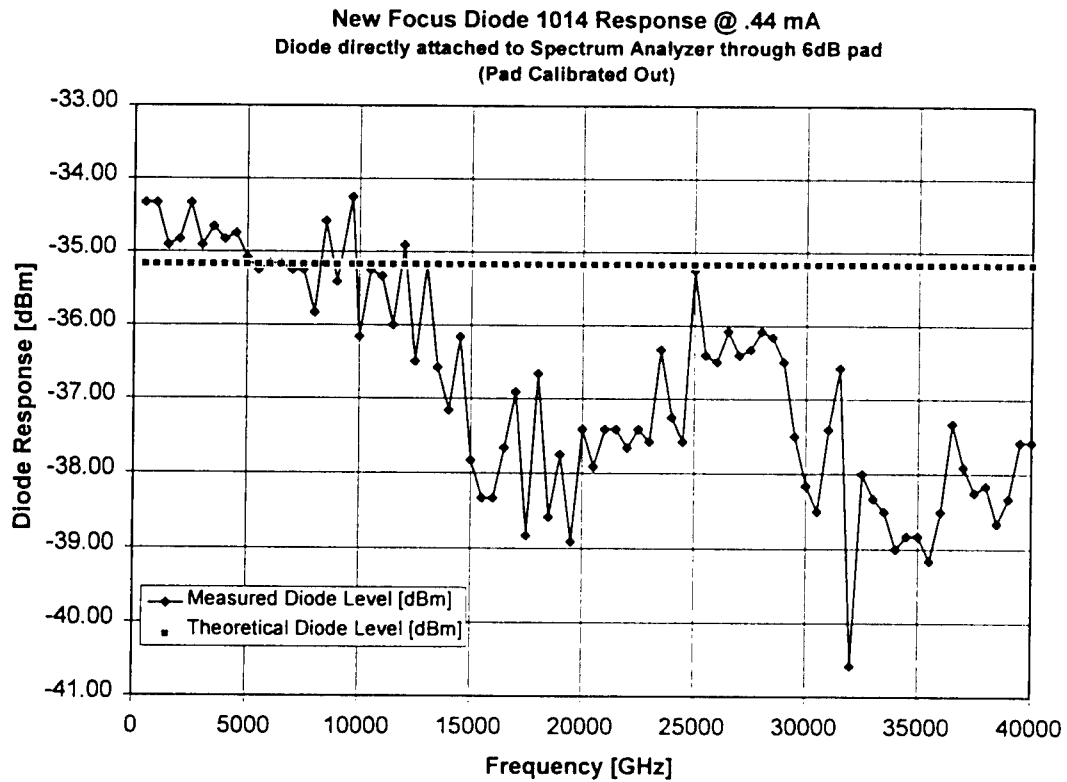
New Focus Diode 1014 Response @ .44 mA
Diode directly attached to Spectrum Analyzer through 6dB pad
(Pad Calibrated Out)

Figure 10. Frequency response of the New Focus photodiode. This data is subtracted from the raw data of Figure 9 to obtain the actual response of the Mach-Zehnder modulator.

Block Frequency upconversion data
NRL MZ 13Z43B (Vpi=7.8 V@ 2GHz), 50 ohm New Focus 1014 (.56 mA), 6dB pad (calibrated out)
Optical LO=40.5 GHz, Low sideband

11a) Upconversion

Block Frequency Downconversion Data
NRL MZ 13Z43B (Vpi=7.8 V@ 2GHz), 50 ohm New Focus 1014 (.56 mA), 6dB pad (calibrated out)
Optical LO=40.5 GHz, Low sideband

11b) Downconversion
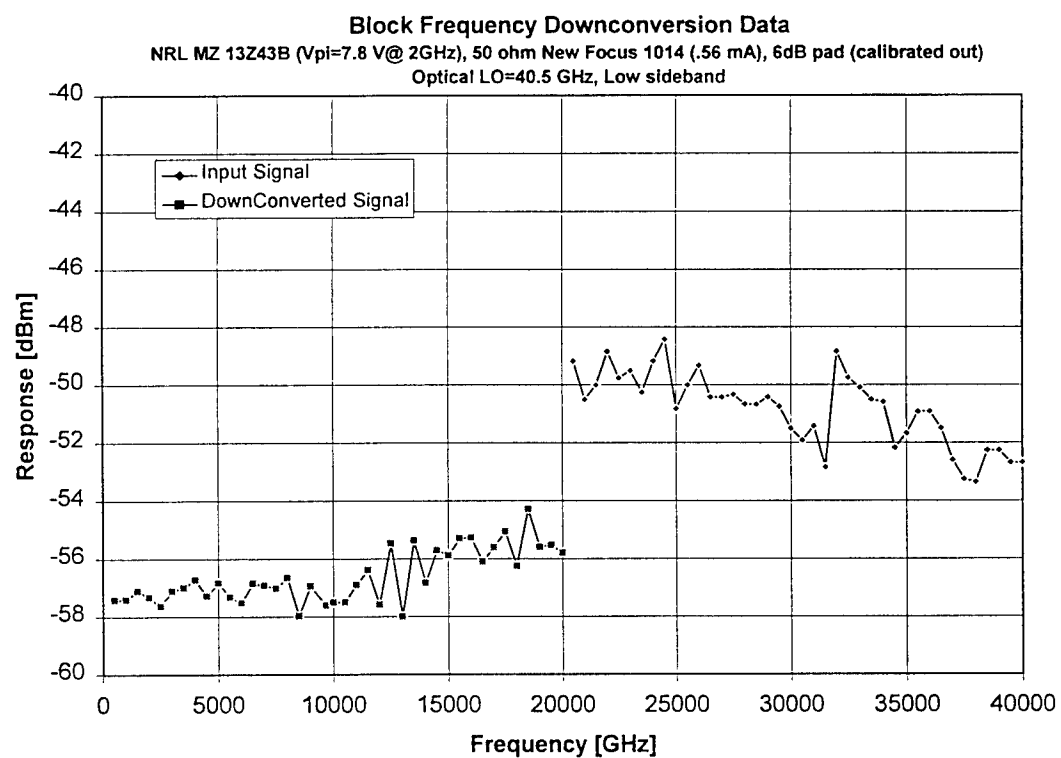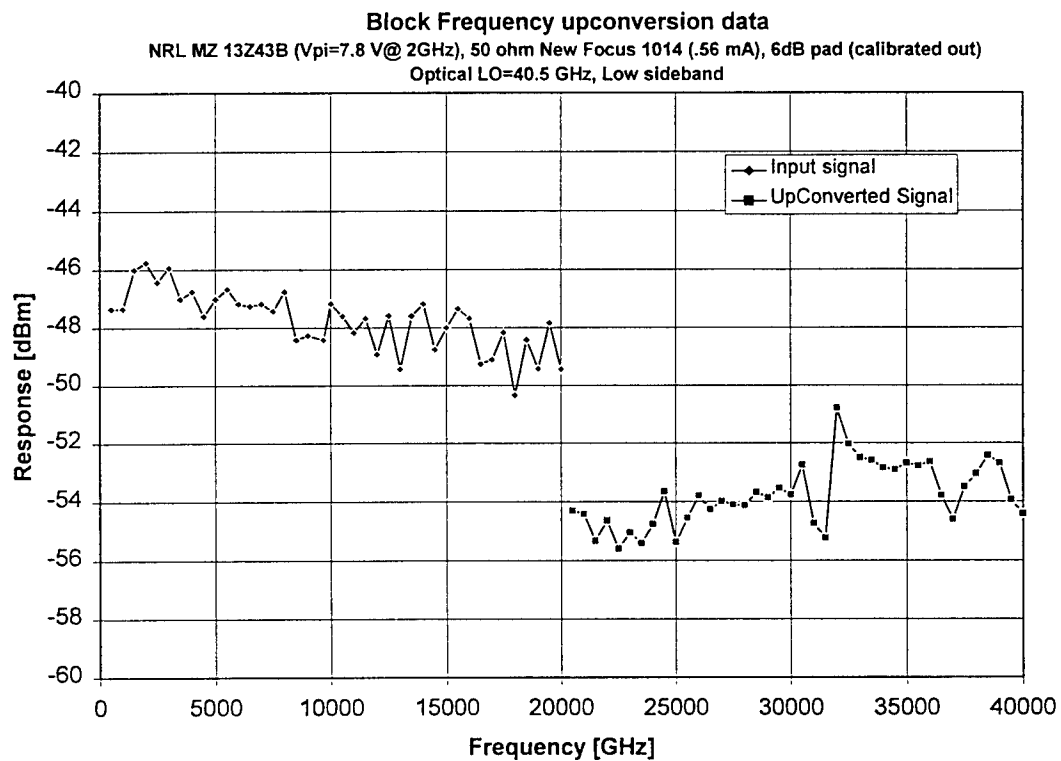
Figure 11. Measured IF and RF data, after correcting for response of photodiode.

Conversion Gain
New Focus Photodiode at Ipd=.56mA
LO=40.5 GHz, Low side RF
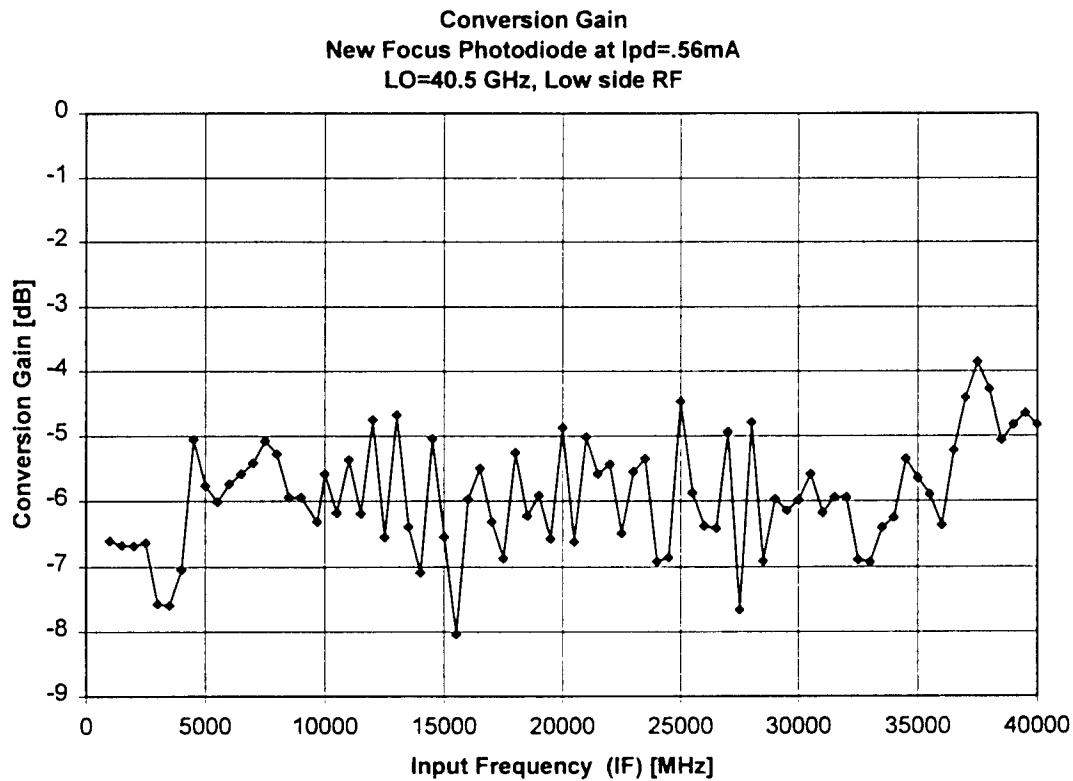
Figure 12. Measured conversion gain of two laser photonic converting system.

```
+4 dBmo
┌──────────────────┐   ┌─────────┐      ┌────────────┐   ┌─────────────┐   ┌──────────────┐
│                  │   │ Optical │      │            │   │  RF Low     │   │  Spectrum    │
│ Unit Under Test  │───│ Atten.  │──────│ Photodiode │───│  Noise Amp  │───│  Analyzer    │
│                  │   │         │      │            │   │             │   │              │
└──────────────────┘   └─────────┘      └────────────┘   └─────────────┘   └──────────────┘
```

JDS la1553-FAS   Lasertron QDMH3 or   Miteq   HP8563E
or Equivalent   Equivalent   AMF-4D-005220-35-10P or Equivalent
                                           or Equivalent
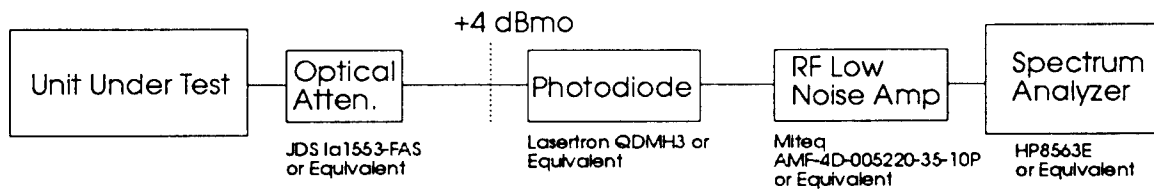
Figure 13. Experimental setup used to measure noise figure of link. (QDMH3 photodiode internal impedance equals 1K ohm, DC photocurrent equals 3 mA.)

Measured Noise Floor for two laser photonic converter system
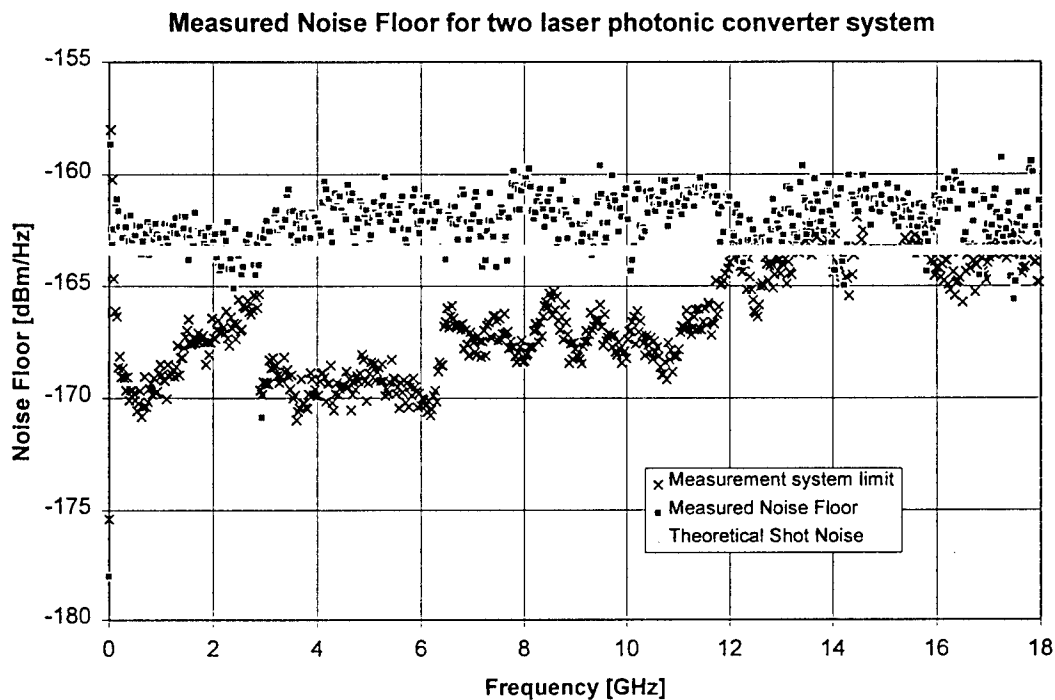
Figure 14. Measured noise floor of two laser photonic converting system.

Noise Figure
NRL MZ 13Z43B (Vpi=7.8 V@ 2GHz), 50 ohm New Focus 1014 (.56 mA), 6dB pad (calibrated out)
Optical LO=40.5 GHz, Low sideband
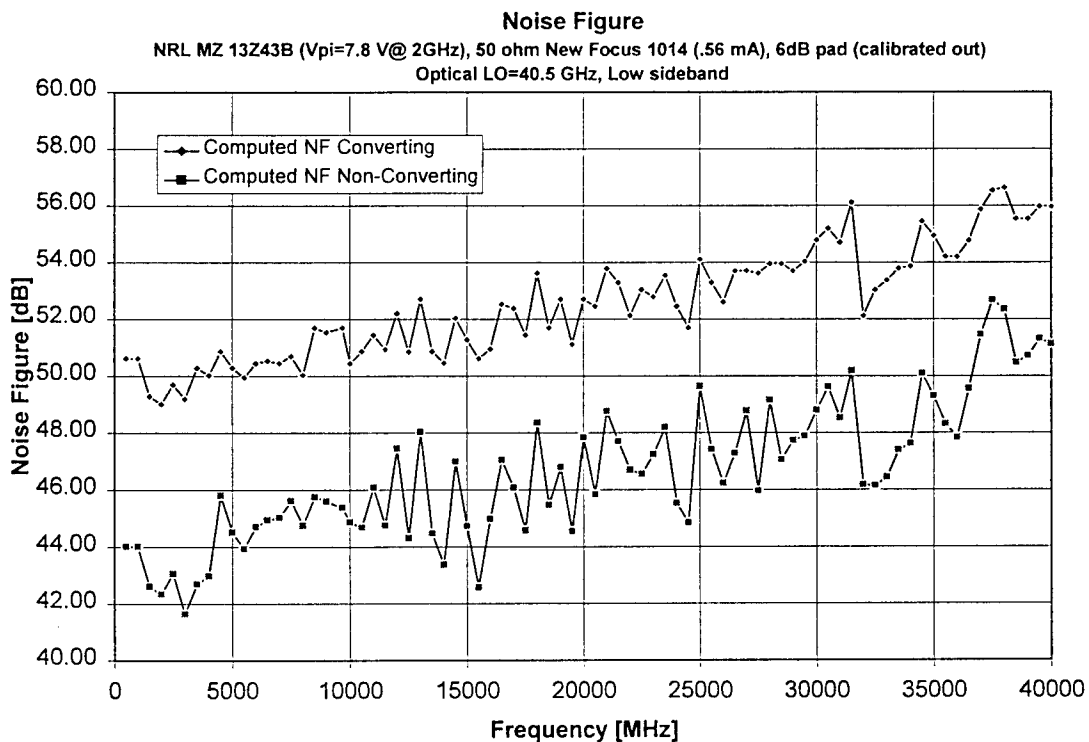
Figure 15. Noise figure of non-converting and converting link.

HP83650B

RF Signal Generator

TRAK 60A3401

Isolator

RF Signal Generator

Isolator

TRAK 60A3401

HP83751B

Diplexer

K&L Diplexer
51Z10-DC/TC4000-0/0
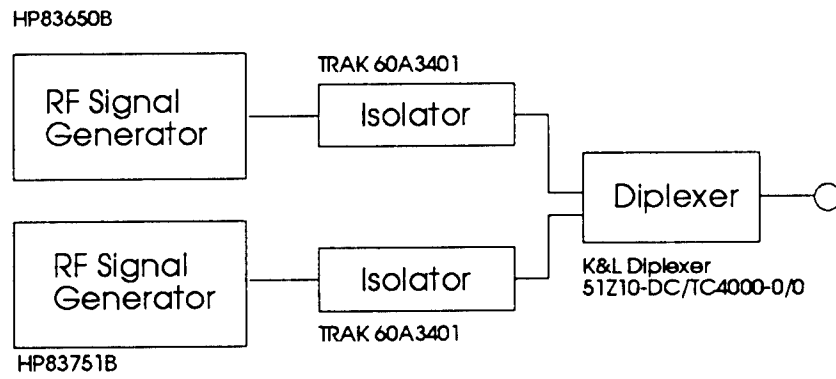
Figure 16. Experimental setup for measuring third order intercept point.

Output IP3 of Frequency Converting Link
NRL MZ 13Z43B, 50 ohm New Focus (.56 mA), 6 dB pad (calibrated out)
(Theoretical Value = -24.1 dBm)

17a. output IP3

Input IP3 vs Frequency
NRL MZ 13Z43B, 50 ohm New Focus (.56 mA), 6 dB pad (calibrated out)
(Theoretical Value = -25.6 dBm @ 3 GHz)
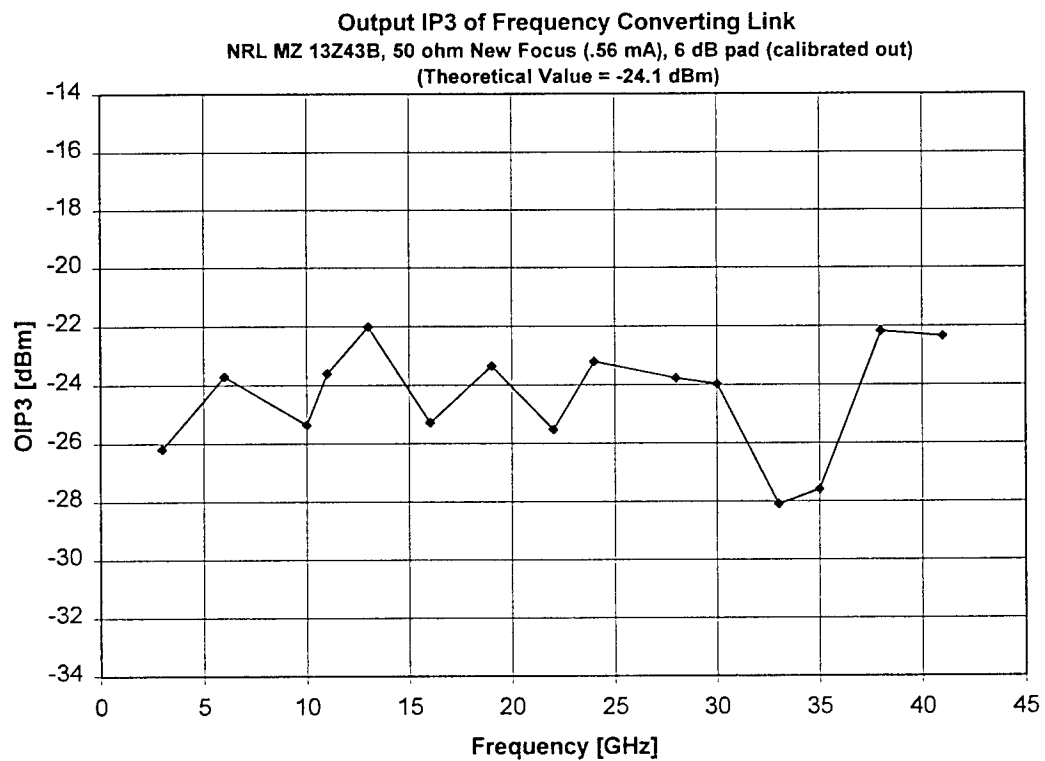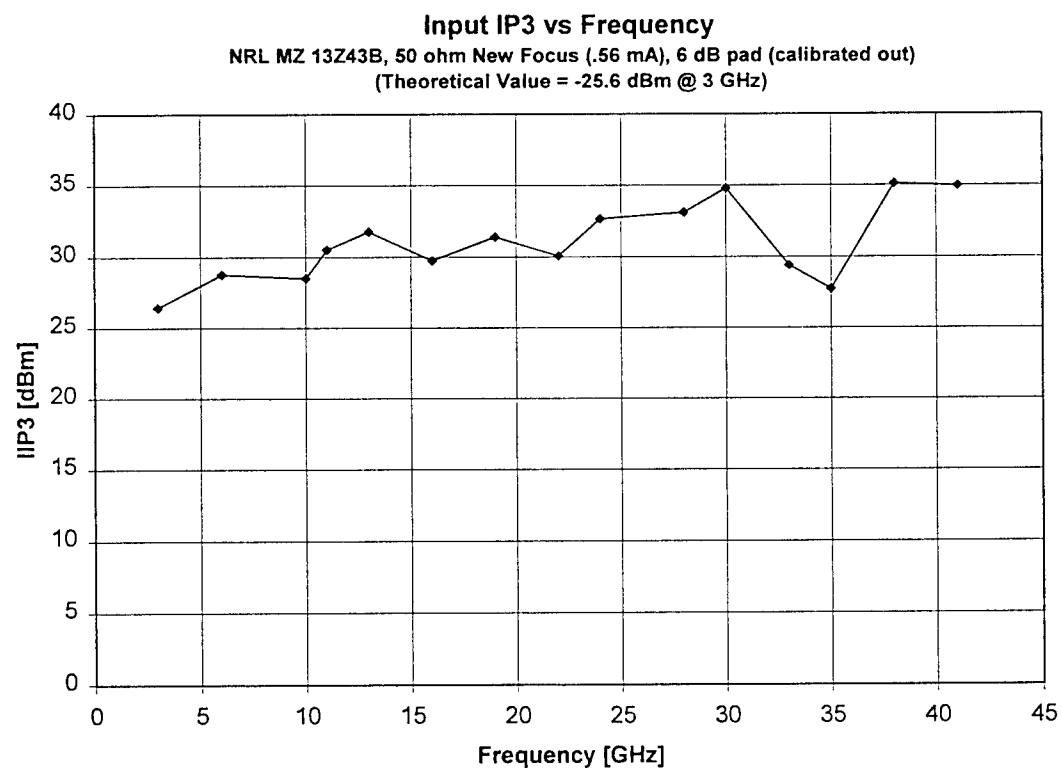
17b. input IP3

Figure 17. Output and input IP3 for the lower side band of the upconverted signal.

33

Return loss of NRL Mach-Zehnder modulator
(Serial Number 13Z43B)
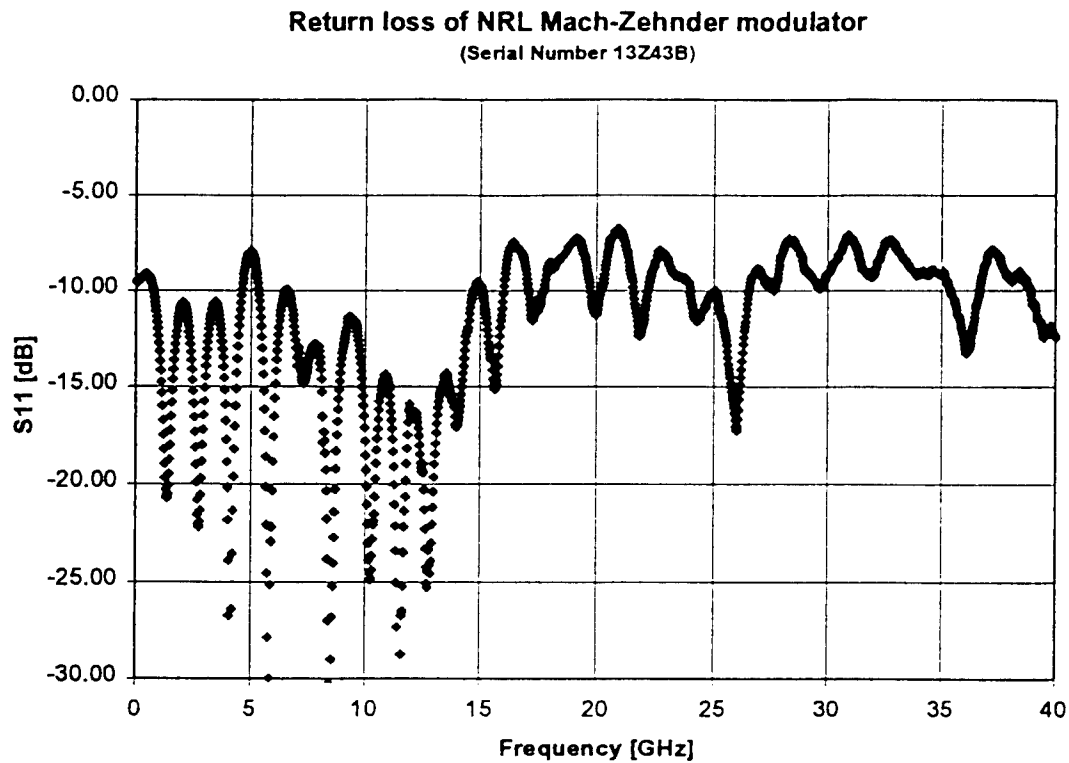
Figure 18. Return loss of the NRL Mach-Zehnder modulator.

Return loss of New Focus Photodiode
(Model 1014, Serial Number 0902)
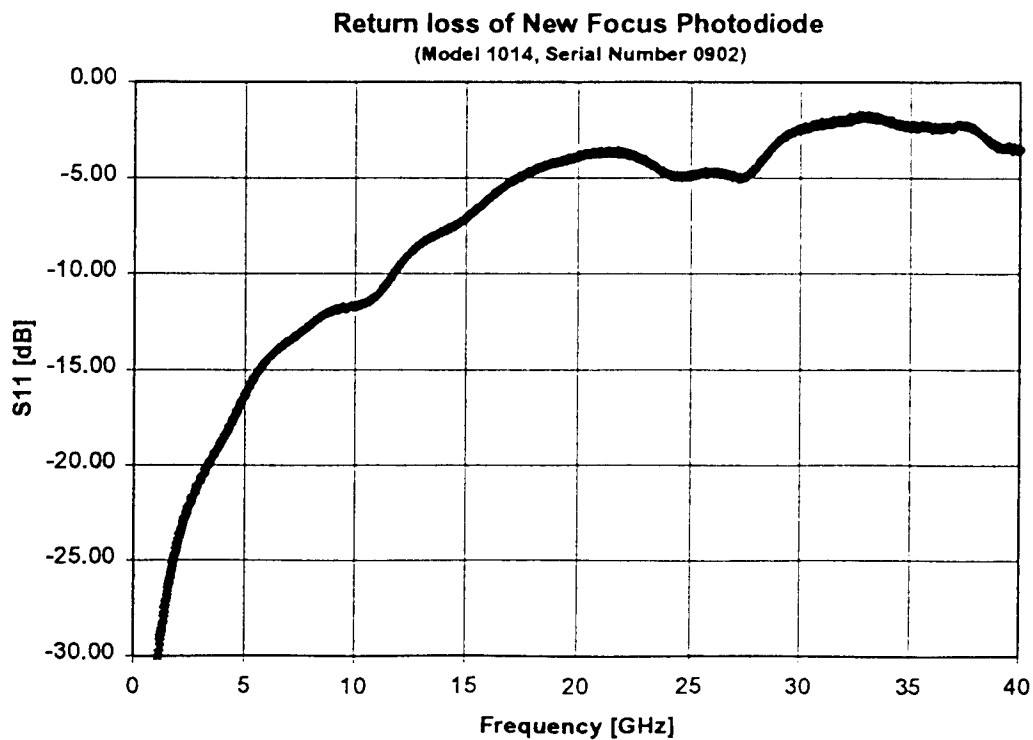
Figure 19. Return loss of the New Focus Photodiode.

Frequency Converting System Phase Noise

NRL MZ (Vpi=7.8V @ 2GHz), 50 ohm NewFocus 1014 (.56 mA)
Upconversion Input=1GHz , LO=37 GHZ, Converted=38 GHz
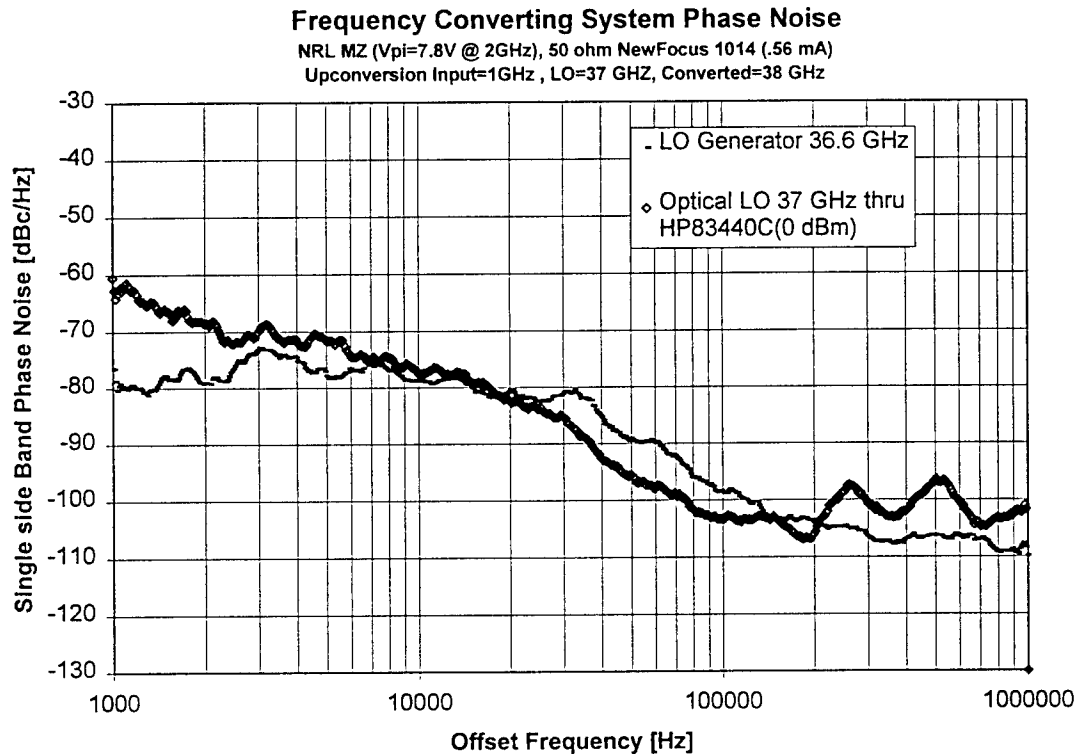
Figure 20. Phase Noise of the reference LO generator and the detected optical LO.

Frequency Converting System Phase Noise

NRL MZ (Vpi=7.8V @ 2GHz), 50 ohm NewFocus 1014 (.56 mA)
Upconversion Input=1GHz , LO=37 GHZ, Converted=38 GHz
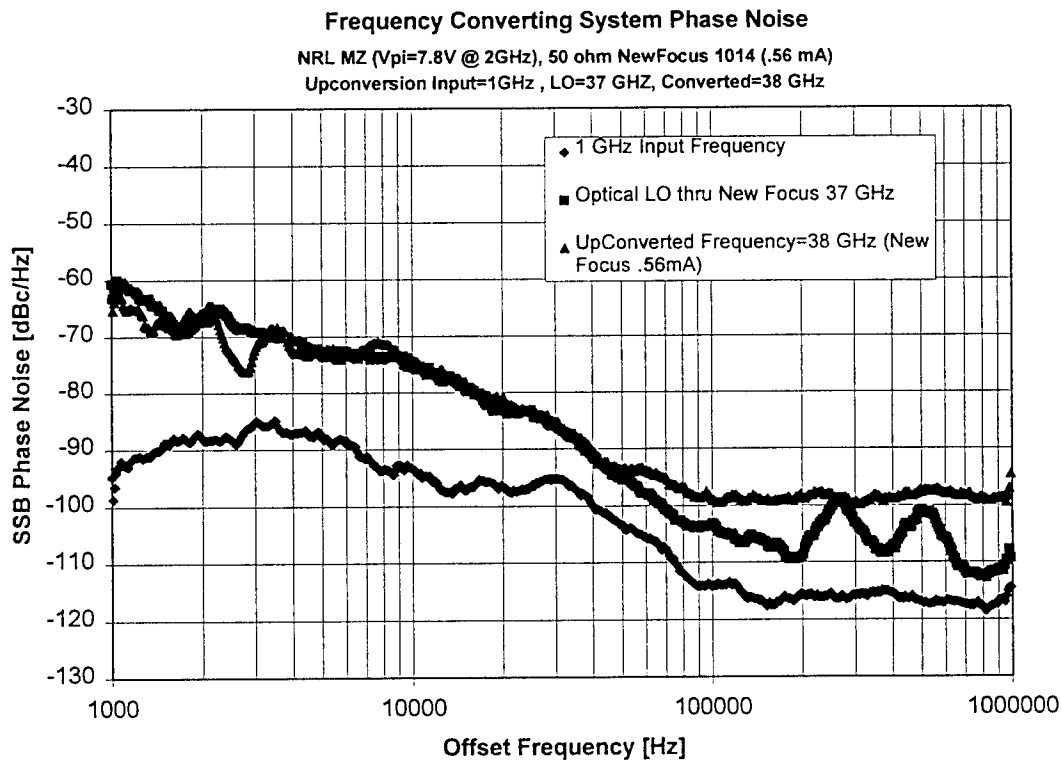
Figure 21. Phase noise of the IF generator, the detected optical LO, and the upconverted signal.

35

EXECUTIVE SUMMARY

This supplement to the Final Report documents additional work done by Tracor exploring the theoretical and experimental results obtained for a wideband electrical heterodyne, photonic down-conversion system. These analyses augment the primary focus of this program which was photonic heterodyne frequency conversion. The system studied consists of a single laser used to feed a pair of Mach-Zehnder modulators (MZM) connected in parallel. The output of the two MZM are mixed using a 2×2 coupler then detected with a balanced photodetector. A local oscillator (LO) tone is fed to one of the MZM while the signals to be converted are fed to the other MZM. The photodetection process generates a signal at the intermediate frequency determined by the frequency difference between the LO and signal frequencies. Analysis of the performance of the parallel MZM link is compared to a cascaded MZM down-converting link using theoretical and experimental methods.

This appendix contains two technical papers that describe the operation and performance of the parallel MZM link. The first paper entitled "Millimeter Wave Frequency Converting Fiber Optic Link Modeling and Results" was presented at the SPIE annual meeting in San Diego, CA on 30 July 1997. The second paper entitled "Comparison of Series and Parallel Optical Modulators for Microwave Down-Conversion" has been submitted for publication to *IEEE Photonics Technology Letters*.

Reprinted from

Optical Technology for Microwave Applications VIII

SPIE

P

PROCEEDINGS
SERIES

Volume 3160

Millimeter Wave Frequency Converting Fiber Optic Link Modeling and Results

J. T. Gallo, K. D. Breuer, and J. B. Wood

Tracor Aerospace Electronic Systems, Inc.
305 Richardson Road
Lansdale, Pennsylvania 19446 USA

ABSTRACT

A down-conversion photonic link implemented with a pair of parallel Mach-Zehnder modulators has been demonstrated. The block down-converter has a fixed local oscillator at 22 GHz and has demonstrated conversion of the 26-40 GHz millimeter-wave band down to the 4-18 GHz microwave intermediate frequency band. A conversion efficiency improvement over down-conversion links with serial modulator topologies with comparable components is predicted.

Keywords: Fiber Optic Link, Down-Converter, RF Mixing

1. INTRODUCTION

Remotely located antennas for the millimeter-wave frequency band are difficult to implement directly as they require broadband electrical connections that may run up to several tens of meters. This limitation is typically mitigated by placing multi-stage down-converters at the antenna front-end to obtain intermediate frequencies (IF) that are more amenable to transmission over conventional coaxial cable. A block diagram of a representative down-converted millimeter-wave link is shown in Figure 1a. The two stepped local oscillator (LO) down-converters in the link are usually located at the front end, while the final, tuned LO down-conversion to the processing IF occurs at the receiver.

Advances in microwave fiber optic links have led to their insertion as a transmission medium after the millimeter-wave signal has been down-converted to the microwave band. Such an insertion is shown in Figure 1b. Recent improvements in the bandwidth and performance of electro-optic modulators has enabled millimeter-wave fiber optic links (see Figure 1c). This allows reasonable signal transmission distances without requiring down-converters at the antenna front-end. Down-conversion is still required, but may be handled at the in-board receiver/processor.

The electrical field produced at the output of a photodetector is proportional to the square of the incident optical power. Knowledge of this relationship has led researchers to investigate ways to achieve at least one of the required down-conversions photonically using the photodetector as a mixer. Removing the need for the highest frequency down-converter in the link represents a potential savings in both weight and complexity at the antenna front-end.

Gopalakrishnan et al.[1] reported using a pair of electro-optic Mach-Zehnder modulators (MZM) in series to produce down-converted signals at the photodetector output of a fiber optic link. Subsequently, researchers have added optical amplifiers[2,3] and photodetector impedance matching[4] to improve the down-conversion efficiency. Sun et al.[5] demonstrated LO generation by overdriving the first MZM with reduced signal conversion loss. In these links, the local oscillator signal was applied to the first MZM and the signal to be down-converted was applied to the second MZM. The link configuration for a series MZM down-converter is shown in Figure 2a.

Other conversion methods exist including 1) electrical combination of the LO and signal onto a common MZM,[1] 2) directly modulating the laser with an LO and adding the signal with an external modulator, 3) generation of the LO by beating two laser wavelengths together before the light is modulated with an MZM,[6] and 4) conventional coherent fiber optic link techniques for heterodyne reception. The first method
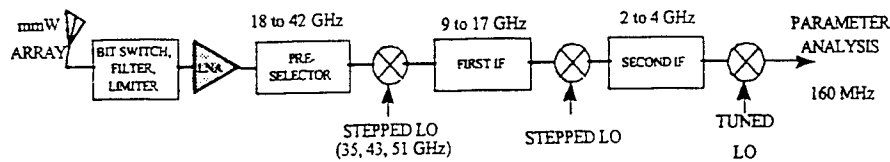
a) electronic mmW link
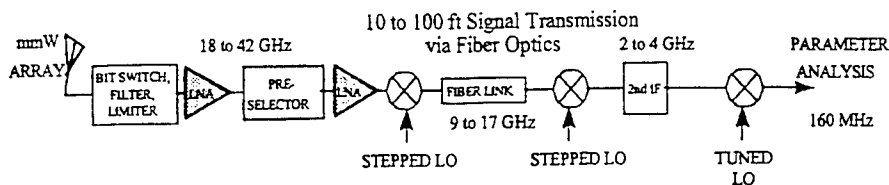
b) fiber optic microwave link
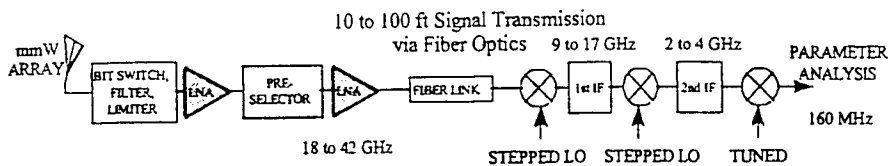

c) fiber optic mmW link

Figure 1. Block diagrams of millimeter-wave down-converting links using a) contemporary electrical links, b) fiber optic microwave links, and c) fiber optic millimeter-wave links.

suffers electrical isolation problems and the second is limited by the modulation frequency available for direct modulation lasers. Dual wavelength techniques require elaborate phase locked loops for proper operation and stabilization of the laser offset frequency. Therefore, the best performance for a stable down-conversion link to date has been achieved with the single carrier, series MZM configuration.

This paper presents a single carrier millimeter-wave down-converter topology based upon two MZMs in a parallel configuration as shown in Figure 2b. The LO is applied to one MZM and the millimeter-wave signal to the other. The modulators are low-biased and fed coherently from a single laser that is split between the LO and signal MZMs. Proper optical phase control during the quadrature recombination of the MZM outputs provides, in theory, greater than 10 dB improvement in down-conversion efficiency over the series-MZM converters when the same optical components are used for both systems.

2. THEORY

Parallel MZMs have been used for analog fiber optic link linearization[7] and double-sideband, suppressed carrier (DSSC)[8] signal generation. In the former case, signals of the same frequency but different amplitudes are fed into the two modulators biased π out of phase[9] then the output of the MZMs is combined in quadrature. The DSSC device has an RF signal applied to only one MZM and the other is used for amplitude control. The modulator outputs are again combined in quadrature and the MZMs are biased at quadrature. Down-conversion parallel MZMs require quadrature combination of the individual MZM outputs to achieve maximum conversion efficiency, however, the MZM are low-biased.
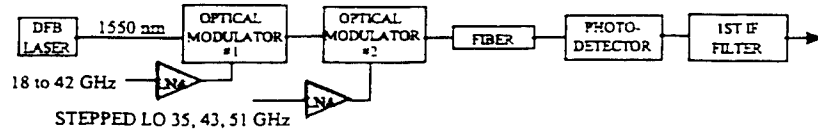
a) series MZM down-converter
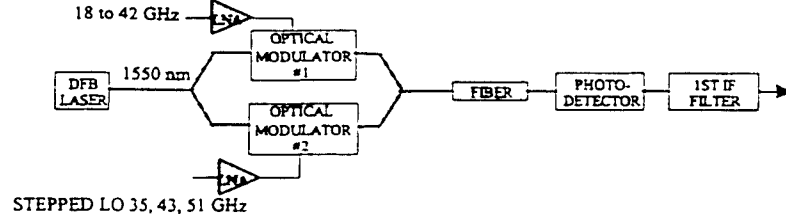
b) parallel MZM down-converter

Figure 2. Millimeter-wave down-converting fiber optic links based upon a) series and b) parallel modulator configurations.

A parallel modulator pair may be fed either coherently or incoherently.[9] In a coherently fed system, optical power from a single laser is split to feed each modulator. Strict phase control between the output of the two modulators must be achieved to maximize the conversion efficiency. The optical phase must be maintained to assure their recombination in quadrature to maximize the down-conversion efficiency. Incoherently fed systems may neglect the variance of phase between the two modulators, however, this benefit is offset by the complex frequency locking required between the two lasers in the incoherent topology. Based on these arguments, a coherent approach was adopted.

Consider three links that are comprised of identical components. Figure 3a shows a direct millimeter-wave fiber optic link with no down-conversion. A laser diode which launches an optical intensity of I_o into a fiber is connected to a MZM modulator with a 7 dB insertion loss, 3 dB of loss for the connectors, and 3 dB resulting from the quadrature bias point set for the device. These loss values are relatively high, but are representative of experimental results. The modulated light is incident on a photodetector of responsivity, $\Re$. In traversing the link, the fiber-coupled laser output suffers a loss α_{dir}. The detected output power into a 50 Ω load at the signal frequency, ω_{sig}, is given by the equation

$$P(\omega_{sig}) = \frac{50\left(\Re\alpha_{dir}I_o/2\right)^2}{2}\left[2J_1\left(2\beta_{sig}\right)\right]^2 \tag{1}$$

where $J_1(\beta)$ is the first order Bessel function of the first kind,

$$\beta = \frac{\pi}{V_\pi}\sqrt{\frac{R}{2}10^{(P-30)/10}}, \tag{2}$$

V_π is the modulator half-wave voltage, R is the modulator input resistance, and P is the input signal power in dBm.

Similar equations may be derived for the series MZM (quadrature bias) and parallel MZM (low-bias) down-converting links shown in Figures 3b and 3c. The detected electrical power into a 50 Ω load at the down-conversion frequency, $\omega_{sig} - \omega_{lo}$, is

$$P(\omega_{sig} - \omega_{lo}) = \frac{50\left(\Re\alpha_{ser}I_o/2\right)^2}{2}\left[2J_1(\beta_{sig})J_1(\beta_{lo})\right]^2 \tag{3}$$
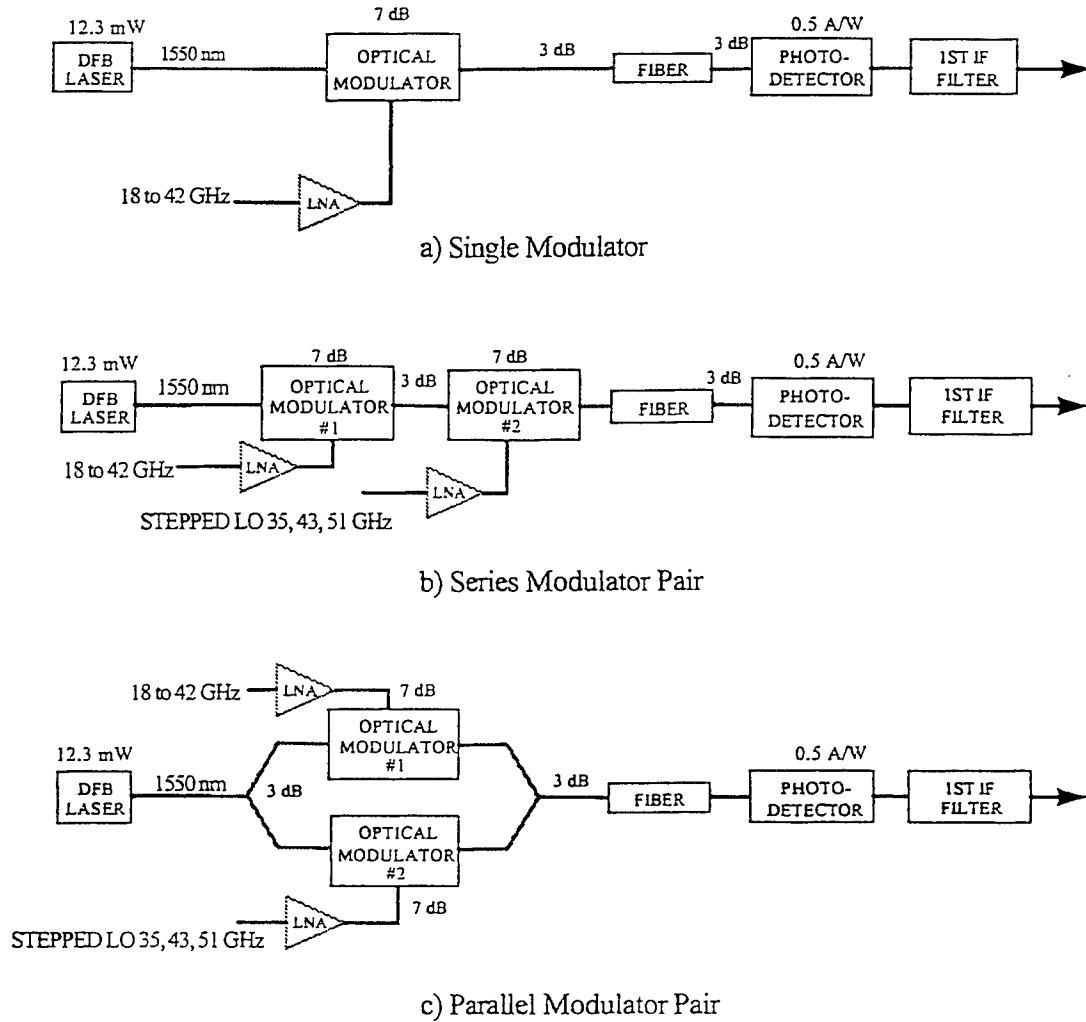
Figure 3. Link topology for a) direct millimeter-wave fiber optic link, b) series modulator down-converting link, and c) parallel modulator down-converting link. Identical components are used in each link to compare their performance.

for the series down-converter and

$$P(\omega_{sig} - \omega_{lo}) = \frac{50\,(\Re\alpha_{par}I_o)^2}{2}\,[J_1(\beta_{sig})J_1(\beta_{lo})]^2 \tag{4}$$

for the parallel down-converter.

Assuming that the same laser, detector and modulators are used in each of these three links enables a direct comparison for anticipated link performance. Furthermore, the serial and parallel converters may be compared with a standard fiber link with electronic down-conversion. The plot in Figure 4 shows a comparison of the received IF power resulting from down-conversion as a function of the LO power using the serial and parallel links. The received power from a millimeter-wave fiber optic link followed by a typical single-stage electronic down-converter with 15 dB conversion loss is also shown. Using the same MZMs for both the serial and parallel converters, the parallel converter should have at least 15 dB better conversion efficiency ($\alpha_{dir} = 13$ dB, $\alpha_{ser} = 20$ dB, and $\alpha_{par} = 13$ dB). This efficiency will exceed that for a conventional fiber link with electronic conversion when the LO power is greater than 16 dBm.
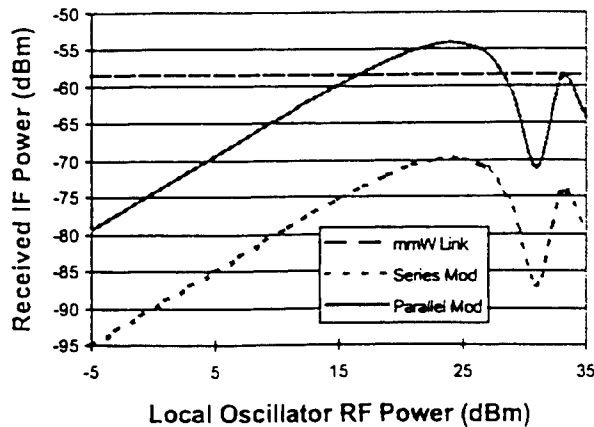
Figure 4. Comparable received power at the first IF for series and parallel down-converting links as function of the LO power applied to the modulator. Performance of a millimeter-wave fiber optic link followed by an electronic down-converter (with 15 dB of conversion loss) is plotted for a baseline. V_π for the modulators was assumed to be 6 volts at 22 GHz and 9 volts at 40 GHz based upon a device used in the next section.

3. EXPERIMENTAL RESULTS

The experimental setup is shown in Figure 5. Polarization-maintaining (PM) fiber is required throughout to assure optimum mixing of the two MZM outputs. A Lightwave Nd:YAG Model 125 solid-state laser with a fiber-coupled output power of 23 dBm was connected to a 90:10 splitter. The 90-coupling leg was input to a Sumitomo TMZ13-04 MZM that was low biased. This modulator received the millimeter-wave signal to be converted. Frequencies used ranged from 26 GHz to 40 GHz. The output of the Sumitomo modulator was pigtailed to single-mode fiber so a polarization controller and polarizer were required to connect the modulator to the PM 50:50 splitter.
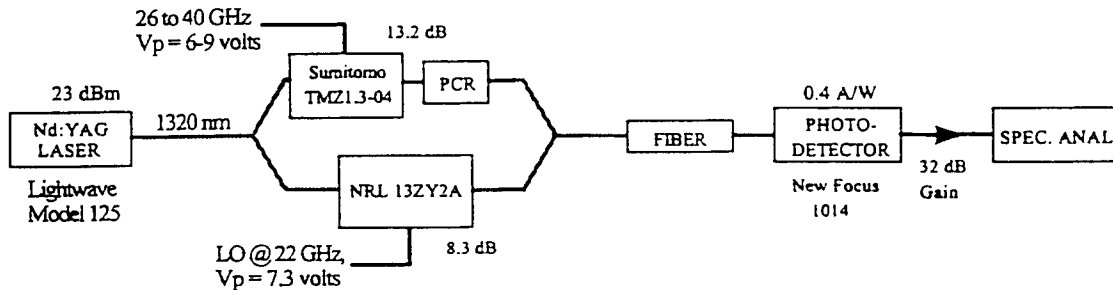

Figure 5. Experimental parallel down-conversion link is shown. The average optical power at the detector when both MZM are low-biased is 0.025 mW. The Sumitomo modulator has single-mode fiber on the output which requires a polarization controller and polarizer (PCR). A 32 dB gain RF amplifier is located between the photodetector output and the spectrum analyzer. The optical throughput loss for each modulator arm is shown.

The 10-coupling leg of the input splitter was input to an NRL 13ZY2A MZM that was low-biased and received the LO modulation. This modulator had PM input and output fiber so no polarization controller was required. The output of both modulators was combined and detected using a New Focus 1014 high-frequency detector. The detector output was passed through a 32 dB gain amplifier and observed with

a spectrum analyzer. Alignment of the optical phase between the two modulator outputs was adjusted manually by repositioning the fiber on the optical bench. This method was tedious and produced reasonable results only in conjunction with the *maximum hold* feature of the spectrum analyzer.

Data was taken to show the down-conversion of the 26-40 GHz band with a fixed LO of 22 GHz. The electrical power in the LO was 7 dBm measured at the input to the MZM which has a $V_\pi = 7.3$ volts and an input impedance of 35 Ω ($\beta_{LO} = 0.127$ radians). The polarization controller was set to maximize the throughput of the polarizer. The detected IF signal ranged in frequency from 4-18 GHz is shown in Figure 6. The photodetector response is flat across this band, however, the RF amplifier following the detector was not which is evident in the figure. Also, the frequency synthesizer used for generating the millimeter-wave input signal had a roll-off in its response from 26-40 GHz which contributed to the decay with frequency. The theoretical (solid curve) data in the Figure reflect the synthesizer response by not that of the amplifier.
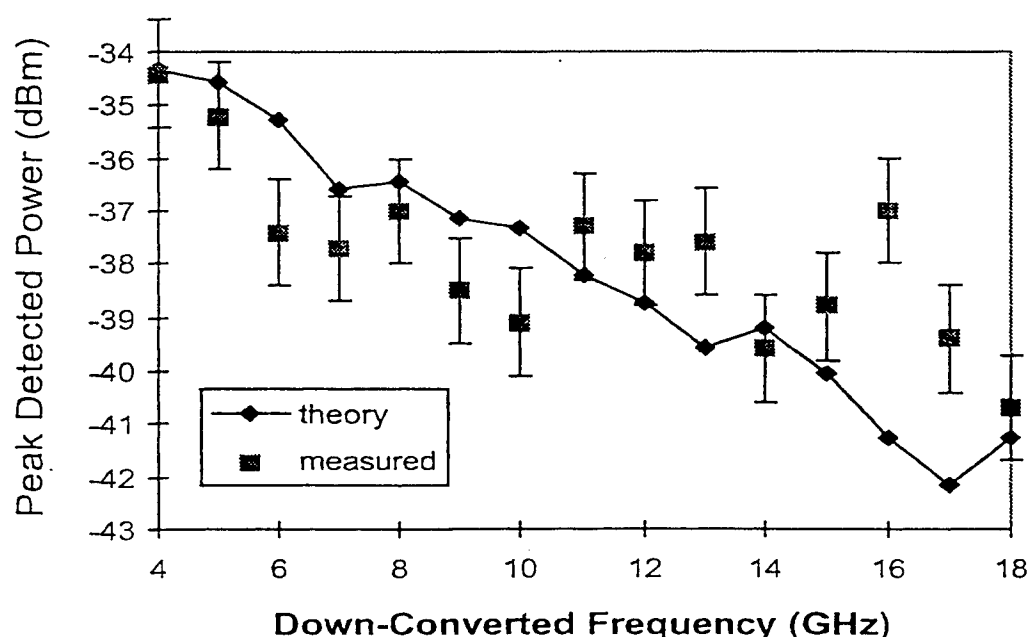

Figure 6. Conversion loss versus down-converter frequency is shown. An RF amplifier of 32 dB gain was placed between the photodetector and the spectrum analyzer. The mean optical power on the detector was 25 microwatts.

Dynamic range of the converting link was not measured, however, some data was taken to determine the relationship of the detected IF to the signal power for several LO levels. This data is shown in the plot of Figure 7. The expected linear relationship between the input signal power and the detected IF power is evident in the Figure.

4. CONCLUSIONS

Initial modeling of the proposed parallel MZM down-converter shows a potential 10-15 dB improvement in conversion efficiency compared to series MZM down-converters. The techniques has been demonstrated in the laboratory albeit without automated control of the modulators' bias points, polarization controller, or relative phase between the output of the two modulators. These limitation not withstanding, conversion data comparable to that reported for series converters (without optical amplifiers or impedance matching)
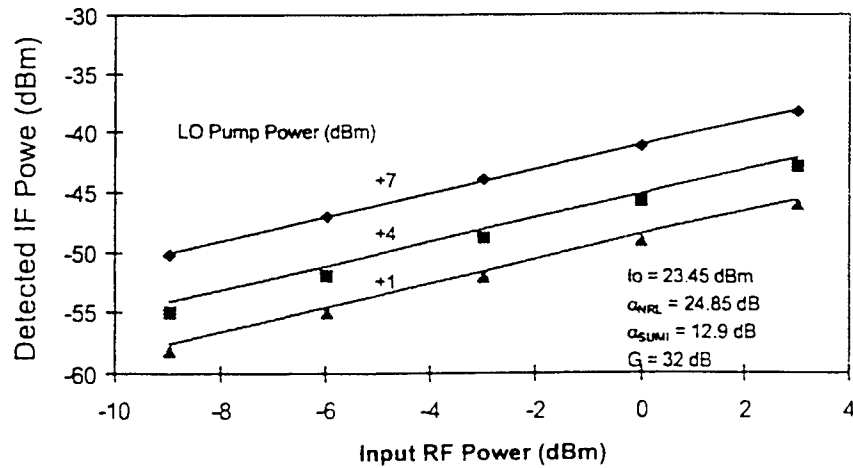
Figure 7. Detected IF power versus the input signal power is shown for several LO input levels. All powers are electrical into a 50 Ω load. The optical loss from laser through each modulator (α_{nrl} and α_{sumi}) to the photodetector is shown.

was obtained. Removing the 32 dB RF gain of the amplifier, a conversion loss of 66-72 dB across the 26-40 GHz signal band was obtained with an LO power of only 7 dBm.

The primary advantage of the parallel down-converting link over series modulator implementations is due to the reduced link loss. This benefit comes at the expense of requiring a phase locking loop to adjust the relative phase between the parallel modulators. The tracking rate required (on the order of milliseconds) for this phase loop is substantially less than that required for the dual wavelength down-converting systems (less than 1 nanosecond). The improved conversion efficiency may offset this added complexity for some applications. Furthermore, the parallel configuration lends itself more readily to integration than the series configuration, especially in the millimeter-wave band where long (several centimeters) MZM electrodes are required to achieve reasonable V_π values.

Experimental comparison of the parallel link with a series link to verify the theoretical predictions presented here is warranted. Thereafter, inclusion of conversion efficiency enhancement techniques such as the use of optical amplification and over-driving modulators may be considered. It is expected that results should improve upon current results reported with series down-converters.

ACKNOWLEDGEMENTS

REFERENCES

1. G. Gopalakrishnan, W. K. Burns, and C. H. Bulmer, "Microwave-optical mixing in linbo$_3$ modulators," *IEEE Transactions on Microwave Theory and Techniques* 41, pp. 2383–2391, 1993.
2. G. K. Gopalakrishnan, R. P. Moeller, M. M. Howerton, W. K. Burns, K. J. Williams, and R. D. Esman, "A low-loss downconverting analog fiber-optic link," *IEEE Transactions on Microwave Theory and Techniques* 43, pp. 2318–2323, 1995.
3. K. J. Williams and R. D. Esman, "Optically amplified downconverting link with shot-noise-limited performance," *IEEE Photonics Technology Letters* 8, pp. 148–150, 1996.

4. R. Helkey, J. C. Twichell, and I. C. Cox, "A down-conversion optical link with rf gain," *Journal of Lightwave Technology* 15, pp. 956–961, 1997.

5. C. K. Sun, R. J. Orazi, and S. A. Pappert, "Efficient microwave frequency conversion using photonic link signal mixing," *IEEE Photonic Technology Letters* 8, pp. 154–156, 1996.

6. J. R. T. Logan and E. Gertel, "Millimeter-wave photonic downconverters: Theory and demonstrations," *Proc. SPIE* 2560, pp. 58–69, 1995.

7. J. L. Brooks, G. S. Maurer, and R. A. Becker, "Implementation and evaluation of a dual parallel linearization system for am-scm video transmission," *Journal of Lightwave Technology* 11, pp. 34–41, 1993.

8. D. L. Sipes and E. Gertel, "Wide-dynamic-range optical link using dssc linearization," *Proc. SPIE* 2155, pp. 264–274, 1994.

9. S. K. Korotky and R. M. DeRidder, "Dual parallel modulation schemes for low-distortion analog optical transmission," *IEEE Journal on Selected Areas in Communications* 8, pp. 1377–1381, 1990.

Comparison of Series and Parallel Optical Modulators for Microwave Down-Conversion

J. T. Gallo and J. K. Godshall

Abstract— Photonic down-conversion of microwave signals using a pair of broadband optical modulators is investigated theoretically and experimentally for cascaded and parallel modulator topologies. Parallel links offer up to 14 dB of conversion efficiency improvement over cascaded links. Photodetector saturation is avoided using modulator low-biasing and balanced detection allowing a further improvement of over 20 dB through increased laser power.

I. INTRODUCTION

DOWN-converting fiber optic links for remotely-located antenna applications have received considerable attention in recent years. Single lasers with cascaded, quadrature-biased Mach-Zehnder modulators (MZM) [1] and paired lasers with a single, quadrature-biased MZM [2] are the leading research areas reported. Techniques for improving conversion efficiency of cascaded MZM links include photodetector impedance matching [3], optical amplification with balanced detection [4], [5], integrating the cascaded MZMs [6], overdriving the local oscillator (LO) MZM [7], [8], and low-biasing one of the MZM [9]. Dual laser techniques continue to progress [10], [11], but are not considered here.

Recently, low-biased, parallel MZMs have been employed for fiber optic down-conversion [12] and for spur-free dynamic range improvement [13]. When identical lasers, photodetectors and modulators are used, low-biased, parallel MZM down-converting links exhibit performance superior to quadrature-biased, cascaded MZM links. Advantages realized by parallel MZM down-conversion links include lower DC optical power on photodetectors and easier integration of dual MZMs on a single substrate. Balanced detection [13] is required to suppress the even-ordered intermodulation terms that arise from low-biasing the modulators as well as improving the efficiency of down-converting links.

This paper presents analysis of low-biased, parallel MZM links compared to quadrature-biased, cascaded MZM links. The effect of intermodulation distortion (IMD) resulting from the low-bias condition is mitigated through balanced detection. Performance improvement is verified experimentally. Predicted conversion gain improvement for higher laser powers, without photodetector saturation, is given based upon the lower average optical power in the low-biased, parallel MZM link.

J. T. Gallo and J. K. Godshall are with Tracor Aerospace Electronic Systems, Inc., 305 Richardson Road, Lansdale, PA 19446 USA. E-Mail: jgallo@aes.tracor.com.

II. ANALYSIS OF DOWN-CONVERTING TOPOLOGIES

Block diagrams of a typical analog fiber optic link as well as cascaded MZM and parallel MZM down-converting links are shown in Figure 1. Analyses of cascaded MZM
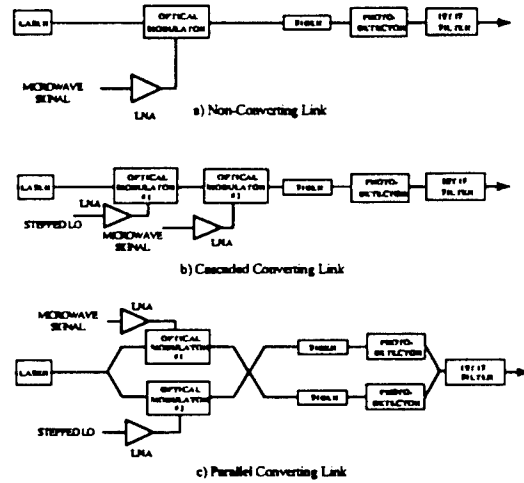

Fig. 1. Block diagrams of fiber optic links using a) typical microwave link, b) cascaded modulator down-converting link, and c) parallel modulator down-converting link.

down-converting links are reported for quadrature-biased MZMs [1], [4] and carrier-suppressed conditions [9]. The cascaded MZM topology requires at least one quadrature-biased modulator to suppress IMD terms. Balanced detection in the parallel MZM topology suppresses IMD levels thereby permitting dual low-biased MZMs with suppressed carrier power.

Photodetector electrical output current in cascaded or parallel MZM links due to a pair of RF tones [14] on the signal modulator, $V_{RF} \sin(\omega_{RF} t)$ and $V'_{RF} \sin(\omega'_{RF} t)$, and a single tone, $V_{LO} \sin(\omega_{LO} t)$, on the LO modulator is [9]

$$
\begin{aligned}
I_o = \ & \Re G_L P_{in} \left[A(0) + A(\omega_{RF}) \sin(\omega_{RF} t) \right. \\
& + A'(\omega'_{RF}) \sin(\omega'_{RF} t) + A(\omega_{LO}) \sin(\omega_{LO} t) \\
& + A(\omega_{IF}) \cos(\omega_{IF} t) + A'(\omega'_{IF}) \cos(\omega'_{IF} t) \\
& + A(\omega_{M1}) \cos(\omega_{M1} t) + A'(\omega'_{M1}) \cos(\omega'_{M1} t) \\
& A(\omega_{M2}) \cos(\omega_{M2} t) + A'(\omega'_{M2}) \cos(\omega'_{M2} t) \\
& \left. + \text{other mixing terms} \right]
\end{aligned}
\tag{1}
$$

where

$$ G_L = T_D/4 \qquad \text{for cascade links,} \tag{2} $$

$$ G_L = 4\sqrt{T_D T_{C1} T_{C2}} \qquad \text{for parallel links,} \tag{3} $$

$\mathfrak{R}$ is the photodetector responsivity, T_D represents optical losses through cascaded modulators, T_{C1} and T_{C2} are the 1×2 and 2×2 coupler composite losses (for an ideal coupler $T_C = 6$ dB which is the composite loss derived from 3 dB of loss per output leg), P_{in} is the fiber-coupled laser optical power, and $A(\omega)$ are the amplitude coefficients of each frequency component, ω. Down-converted signals occur at intermediate frequencies (IF), $\omega_{IF} = \omega_{RF} - \omega_{LO}$ and $\omega'_{IF} = \omega'_{RF} - \omega_{LO}$.

Terms containing ω_{M1} and ω_{M2} are IMD components of significant magnitude that may fall within the band of down-converted signals. In cascaded links, $\omega_{M1} = 2\omega_{RF} - \omega'_{RF} - \omega_{LO}$ when $\omega_{RF} \approx \omega'_{RF}$. The term $\omega_{M2} = 2\omega_{LO} - \omega_{RF}$ when $2\omega_{LO} \approx \omega_{RF}$ [9] and is usually suppressed by biasing both modulators at quadrature in cascaded MZM links or at low-bias for parallel MZM links. In this work, $\omega_{M2} = 3\omega_{LO} - \omega_{RF}$ for cascaded and parallel MZM links.

Amplitude coefficients are given in terms of modulation indices, X_{RF}, X'_{RF}, and X_{LO}. $X_{RF} = \pi V_{RF}/V_{\pi RF}(f_{RF})$ for one RF tone where $V_{\pi RF}(f_{RF})$ is the frequency-dependent half-wave voltage of the modulator. Significant coefficients for low-biased, parallel MZM links are

$$
\begin{aligned}
A(0) &= A(\omega_{RF}) = A(\omega'_{RF}) = A(\omega_{LO}) = 0 \\
A(\omega_{IF}) &= 2J_1(X_{LO}/2)J_1(X_{RF}/2)J_0(X'_{RF}/2) \\
A(\omega_{M1}) &= -2J_1(X_{LO}/2)J_2(X_{RF}/2)J_1(X'_{RF}/2) \\
A(\omega_{M2}) &= 2J_3(X_{LO}/2)J_1(X_{RF}/2)J_0(X'_{RF}/2) \quad (4)
\end{aligned}
$$

assuming signals from the two photodetectors are summed π out of phase (i.e., balanced detection). Significant coefficients for cascaded MZM links are

$$
\begin{aligned}
A(0) &= 1 \\
A(\omega_{RF}) &= -2J_1(X_{RF})J_0(X'_{RF}) \\
A(\omega_{LO}) &= -2J_1(X_{LO}) \\
A(\omega_{IF}) &= 2J_1(X_{LO})J_1(X_{RF})J_0(X'_{RF}) \\
A(\omega_{M1}) &= -2J_1(X_{LO})J_2(X_{RF})J_1(X'_{RF}) \\
A(\omega_{M2}) &= 2J_3(X_{LO})J_1(X_{RF})J_0(X'_{RF}) \quad (5)
\end{aligned}
$$

assuming quadrature-bias on both MZM.

Simulation results of the spectra of signals from a cascaded MZM link with dual quadrature-biased modulators [1] and a parallel MZM link with dual low-bias modulators are shown in Figure 2. In these links, $f_{LO} = 6$ GHz, $f_{RF} = 9.5$ GHz (RF1), $f_{RF} = 10.5$ GHz (RF2), $f_{IF} = 3.5$ (IF1) and 4.5 (IF2) GHz, $X_{RF} = X'_{RF} = X_{LO}/2 = 0.1$, $P_{in} = 100$ mW, $T_D = 14$ dB, $T_{C1} = T_{C2} = 6$ dB, $\mathfrak{R} = 0.9$ A/W, and $P_{out} = 50I_o^2/2$. Dominant IMD peaks at $f_{M1} = 2.5$ and 5.5 GHz occur in both spectra, however, the IMD amplitude is a few dB lower in the cascade MZM link compared to the parallel MZM link. The down-converted (ω_{IF}) signal amplitudes are related by the equation

$$
\frac{P_P(\omega_{IF})}{P_C(\omega_{IF})} = 10\log\left(\frac{16T_{C1}T_{C2}}{T_D}\right) \quad (6)
$$

where $P_P(\omega_{IF})$ and $P_C(\omega_{IF})$ are the electrical power in the received IF signal for the parallel and cascaded links,
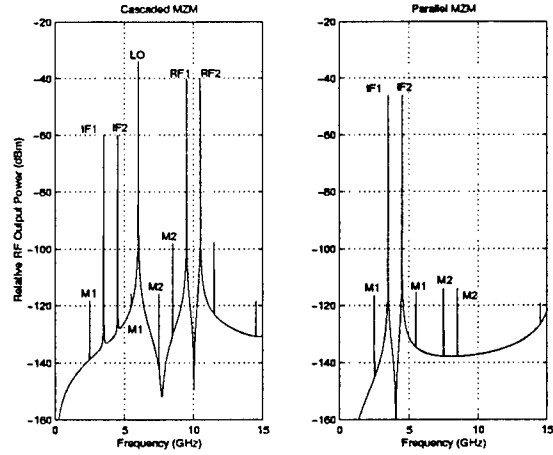

Fig. 2. Frequency content of down-converting cascade (left) and parallel (right) MZM links are shown. System parameters are given in the text. The local oscillator (LO), RF signals (RF1 and RF2), down-converted signals (IF1 and IF2), along with the intermodulation signals (M1 and M2) are indicated.

respectively. Figure 2 shows a 14 dB improvement in the conversion efficiency using the parallel MZM link.

The DC optical power on the photodetector in the quadrature-biased cascaded MZM link is $P_{DC} = T_D P_{in}/4$. Saturation of the photodetector from high P_{DC} limits P_{in} and, subsequently, detected IF power. Low-biased parallel MZMs suppress the DC optical power levels incident on each photodetector in the balanced receiver. The optical DC signal at each photodetector the parallel link is

$$
P_{DC} = \sqrt{T_D T_{C1} T_{C2}} P_{in} \tilde{A}(0) \quad (7)
$$

where

$$
\tilde{A}(0) = 1 - \frac{J_0(X_{LO}) + J_0(X_{RF})J_0(X'_{RF})}{2} \quad (8)
$$

assuming insertion losses of the two optical paths are equal. Combining the photodetector currents out of phase further suppresses this DC component. Each photodetector in the parallel MZM balanced receiver of Figure 2 sees an optical DC power more than 21 dB lower than the single photodetector in the quadrature-biased cascaded MZM link and is only 2 dB higher than the down-converted signal. Therefore, the overall optical power (P_{in}) could be increased by 20 dB, either with additional laser power or an optical amplifier, to improve the conversion efficiency by an additional 20 dB compared to a cascade MZM link.

III. RESULTS

Experimental links were set up having the down-converting topologies shown in Figures 1b and 1c. The same components were used to demonstrate each link. A Lightwave Model 125 Nd:YAG laser with a fiber-coupled output power of 23.3 dBm at 1319 nm fed each link. The LO tone was applied to a high-frequency lithium niobate MZM borrowed from NRL (Model 13ZY2A). The microwave signal was applied to a Sumitomo lithium niobate Model T.MZ1.3-40 MZM. A single photodetector

(Lasertron QDMH1) was used for both links as no suitable balanced detector was available. The responsivity of the photodetector is $\Re = 0.8$ A/W.

LO frequency was fixed in both links at 6 GHz. Signal frequencies at 9.5 and 10.5 GHz were used to explore detected IF and IMD signal strengths. Figure 3 shows the
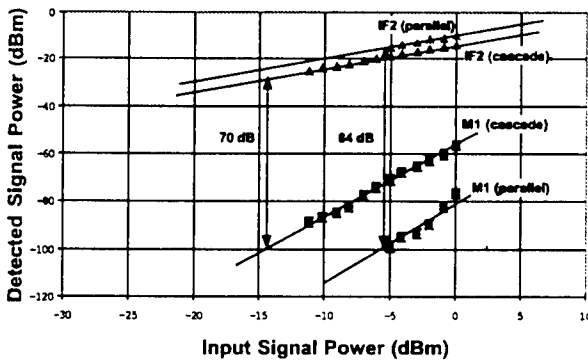

Fig. 3. Measured signal strength of IF2 tones (4.5 GHz) for the cascaded and parallel MZM links are shown. IMD strengths at 5.5 GHz (M1) are also shown. Power applied to the LO MZM was 12.5 dBm at 6 GHz. A 14 dB improvement in spur free dynamic range is demonstrated at -100 dBm noise floor.

detected electrical power of both links as a function of the input RF signal power. Down-converted signals at 4.5 GHz (IF2) in the parallel MZM link were 4 dB stronger than those from the cascaded link. Parallel link IMD at f_{M1} (measured at 5.5 GHz) were suppressed 26-28 dB compared to cascaded MZM link IMD. Increasing the input laser power to the parallel link to generate an average power on the photodetectors equal to that of the cascaded MZM link was not possible due to high optical losses in the components and limited laser power.

This data falls short of theoretical expectations for conversion efficiency improvement of the parallel MZM down-converter. Two deficiencies in the laboratory setup are responsible. The Sumitomo modulator is output coupled using single-mode (SM) fiber while the NRL device uses polarization-maintaining (PM) fiber. Proper mixing of the modulator outputs requires that both MZM are output coupled using PM fiber. A polarization controller and polarizer were required at the Sumitomo output to properly match the polarized output of the NRL device. Monolithic integration of the modulators or PM pig-tailing of both MZMs would avoid this problem. The second problem involves the phase relationship between the two MZM outputs. No attempt was made in the experiment to control these phases resulting in degraded down-conversion efficiency. Phase-locking the MZM outputs, especially when monolithically integrated, is straightforward but increases the complexity of the down-converting link.

IV. CONCLUSION

Results presented in this letter confirm the potential for improved performance of parallel down-converting links compared to cascaded down-converting links that are comprised of the same optical components. Experiments demonstrating the down-conversion of microwave signals showed a 4 dB improvement (out of a theoretical 14 dB improvement) in conversion efficiency for parallel MZM links over cascaded MZM links. Monolithic integration of parallel MZMs is potentially easier than integrated cascaded MZMs and would mitigate optical phase fluctuations in the two paths simplifying phase-locking of the MZM channels. Finally, the parallel approach requires balanced detection thereby limiting the down-conversion bandwidth to that of the balanced detector. Balanced detectors with 10 GHz bandwidth are currently available (from GEC Marconi) which is adequate for many applications.

ACKNOWLEDGEMENTS

REFERENCES

[1] G. Gopalakrishnan, W. K. Burns, and C. H. Bulmer, "Microwave-optical mixing in LiNbO$_3$ modulators," *IEEE Trans. MTT*, vol. 41, pp. 2383–2391, 1993.

[2] R. T. Logan and E. Gertel, "Millimeter-wave photonic downconverters: Theory and demonstrations," *Proc. SPIE*, vol. 2560, pp. 58–69, 1995.

[3] R. Helkey, J. C. Twichell, and C. Cox III, "A down-conversion optical link with rf gain," *J. Light. Tech.*, vol. 15, pp. 956–961, 1997.

[4] G. K. Gopalakrishnan, R. P. Moeller, M. M. Howerton, W. K. Burns, K. J. Williams, and R. D. Esman, "A low-loss downconverting analog fiber-optic link," *IEEE Trans. MTT*, vol. 43, pp. 2318–2323, 1995.

[5] K. J. Williams and R. D. Esman, "Optically amplified downconverting link with shot-noise-limited performance," *IEEE Phot. Tech. Lett.*, vol. 8, pp. 148–150, 1996.

[6] G. K. Gopalakrishnan, W. K. Burns, and C. H. Bulmer, "A LiNbO$_3$ microwave-optoelectronic mixer with linear performance," *IEEE MTT-S Digest*, pp. 1055–1058, 1993.

[7] C. K. Sun, R. J. Orazi, and S. A. Pappert, "Efficient microwave frequency conversion using photonic link signal mixing," *IEEE Phot. Tech. Lett.*, vol. 8, pp. 154–156, 1996.

[8] C. K. Sun, R. J. Orazi, S. A. Pappert, and W. K. Burns, "A photonic-link millimeter-wave mixer using cascaded optical modulators and harmonic carrier generation," *IEEE Phot. Tech. Lett.*, vol. 8, pp. 1166–1168, 1996.

[9] M. M. Howerton, R. P. Moeller, G. K. Gopalakrishnan, and W. K. Burns, "Low-biased fiber-optic link for microwave downconversion," *IEEE Phot. Tech. Lett.*, vol. 8, pp. 1692–1694, 1996.

[10] R. T. Logan, "Photonic radio frequency synthesizer," *Proc. SPIE*, vol. 2844, pp. 311–317, 1996.

[11] X. S. Yao, "Brillouin selective sideband amplification of microwave photonic signals," *IEEE Phot. Tech. Lett.*, vol. 10, pp. 138–140, 1998.

[12] J. T. Gallo, K. D. Breuer, and J. B. Wood, "Millimeter-wave frequency converting fiber optic link modeling and results," *Proc. SPIE*, vol. 3160, pp. 106–113, 1997.

[13] W. K. Burns, G. K. Gopalakrishnan, and R. P. Moeller, "Multioctave operation of low-biased modulators by balanced detection," *IEEE Phot. Tech. Lett.*, vol. 8, pp. 130–132, 1996.

[14] F. Auracher and R. Keil, "Method for measuring the rf modulation characteristics of mach-zehnder-type modulators," *Appl. Phys. Lett.*, vol. 36, pp. 626–629, 1980.